RIGHT ATRIAL DEFORMATION THROUGH SPECKLE TRACKING ECHOCARDIOGRAPHY AND FEATURE TRACKING CMR



Aitzaz Bin Sultan Rai

Green Templeton College

Department of Cardiovascular Medicine

University of Oxford

Status: MSc by Research Student

Supervisors: Prof. Paul Leeson PhD, FRCP, FESC

Prof. Stefan Neubauer MD, PhD, FRCP, FACC, FMedSci

Abstract

The right atrium (RA) plays a vital role in the electromechanical regulation of the heart. Various invasive and non-invasive techniques have been used to elucidate right atrial structure and function. One such novel technique is speckle-tracking echocardiography (STE). Speckle tracking-derived deformation is a relatively new parameter, which is less dependent on loading conditions. STE tracks acoustic scatters (speckles) of myocardium, frame by frame, to calculate the strain or deformation indices of the myocardium. The right atrium is a relatively neglected chamber as it is mostly studied for assessment of atrial mass lesions, congenital and acquired valve lesions and for electro physiological studies. However, its role in the systolic and diastolic function of the right ventricle of the heart has been less explored. I have adapted the STE technique, designed for left ventricular analysis, for use in the right atrial analysis. I undertook a reproducibility study for right atrial deformation parameters and defined normal reference ranges for longitudinal deformation parameters. I have found the analysis approach used generates similar values to those reported in the limited number of previous studies on right atrial STE. I then compared STE derived strain with cardiovascular magnetic resonance feature tracking derived measures of right atrial strain and found moderate agreement between the two techniques. Finally, I investigated whether there are differences in right atrial longitudinal deformation parameters in different patient disease groups. I studied those with Heart Failure with Normal Ejection Fraction (HFNEF) and found a decrease in right atrial function. Whereas, in another cohort of patients with Rheumatoid Arthritis (RhA) there was no statistical difference compared to healthy controls. This thesis

therefore demonstrates the feasibility of using STE to measure right atrial strain and provides evidence that right atrial strain does vary in certain disease conditions.

Keywords

Right atrium, Speckle Tracking Echocardiography, Strain, Feature Tracking Cardiac MRI, Preterm, HFnEF, Inflammatory Cardiomyopathies

Contents

Abstract i

Keywords iii

List of Tables viii

List of Figures ix

Acknowledgements xi

Chapter 1 Introduction 1

1.1 Location 1

1.2 Early History 1

1.3 Anatomy 1

1.3.1 Histology 2

1.3.2 Right Atrial Appendage 2

1.3.3 Crista Terminalis 2

1.3.4 Fossa Ovalis 3

1.3.5 Coronary Sinus 3

1.4 The Right Atrial Physiology 3

1.4.1 The Reservoir Phase 3

1.4.2 The Conduit Phase 4

1.4.3 The Contractile Phase 4

1.5 Assessment Of Right Atrial Structure Through Imaging 5

1.5.1 History of Imaging of the Right Atrium 5

1.5.2 Echocardiography 5

1.5.3 Cardiac MRI 6

1.5.4 MDCT and cineangiography 6

1.6 Assessment Of Right Atrial Function Through Imaging 7

1.6.1 Conventional Echocardiographic Measures 7
1.6.2 Novel Techniques to Assess the Right Atrial Function 7
1.7 Speckle Tracking Echocardiography (STE) 9
1.7.1 Principles of Speckle Tracking 9
1.7.2 Speckle Tissue Architecture or Random Noise 11
1.7.3 Strain Parameters Derived from STE 12
1.7.4 Image Analysis 14
1.8 Applications of STE 15
1.8.1 Hypertension 15
1.8.2 Diabetes 16
1.8.3 Hypertrophic Cardiomyopathy 16
1.8.4 Dilated Cardiomyopathy 17
1.8.5 Restrictive Cardiomyopathy (RM) Vs. Constrictive Pericarditis (CP) 17
1.8.6 Inflammatory Cardiomyopathies 18
1.8.7 Takutsubo Cardiomyopathy 18
1.8.8 Valvular Heart Disease 19
1.8.9 Miscellaneous 19
1.8.10 Emerging Applications 20
1.9 Aim of Research 21
Chapter 2 Methods of Image Acquisition and Analysis 23
2.1 Introduction 23
2.2 System Settings 23
2.3 Image Analysis 24
2.3.1 ACP Toshiba 24
2.3.2 Tomtec 25
2.4 Output 26

Chapter 3 Reproducibility Study for Speckle Tracking-derived Right Atrial Strain 29

3.1 Introduction 29

3.2 Methods 29

3.2.1 Study Population 29

3.2.2 Study Procedure 29

3.2.3 Statistical Analysis 30

3.3 Results 30

3.3.1 Inter-observer Agreement 30

3.3.2 Intraobserver Agreement 32

3.4 Discussion 34

Chapter 4 The Reference Ranges for the Right Atrial Strain 36

4.1 Introduction 36

4.2 Methods 36

4.2.1 Patient Characteristics 36

4.2.2 Statistical Methods 37

4.3 Results 37

4.3.1 Normal Reference Ranges 37

4.4 Discussion 41

Chapter 5 Comparison of Echocardiography and CMR-derived Atrial Deformation Parameters 44

5.1 Introduction 44

5.2 Methods 45

5.2.1 Sample Size 45

5.2.2 Echocardiography Protocol 45

5.2.3 MRI Protocol 45

5.3 Results 47

5.4 Discussion 48

Chapter 6 Right Atrial Strain in Heart Failure with Normal Ejection Fraction 51

6.1 Introduction 51

6.2 Methods 52

6.2.1 Sample Size 52

6.2.2 Study Procedure 53

6.3 Results 54

6.4 Discussion 57

Chapter 7 Right Atrial Strain in Rheumatoid Arthritis 59

7.1 Introduction 59

7.1.1 Rheumatoid Arthritis ..... **Error! Bookmark not defined.**

7.2 Methods 61

7.2.1 Setting 61

7.2.2 Study Procedure 61

7.3 Results 61

7.4 Discussion 65

7.4.1 Main Findings 65

Chapter 8 Conclusions and Future Directions 66

8.1 Conclusions 66

8.2 Future Directions 68

8.2.1 STE Image Quality and Strain 68

8.2.2 Study of Right AV Mechanical Coupling 69

References 71

List of Tables

Table 1.1. Strain parameters 13

Table 3.1. Inter-observer agreement for atrial phasic mechanics through Bland–Altman method. 30

Table 3.2. The intra-observer limits of agreement and bias for right atrial strain 32

Table 4.1. Characteristics of the population 37

Table 4.2. Echocardiographic parameters. 40

Table 4.3. Longitudinal strain parameters for the right atrium 40

Table 4.4. Comparison of right atrial strain values 42

Table 5.1. Demographics of females undergoing CMR examination. 47

Table 5.2. Limits of agreement and bias between strain and SR parameters derived by echocardiography and CMR. 48

Table 6.1. Demographics of the normal cohort 53

Table 6.2. Comparison of various strain parameters between healthy controls and the HFnEF group 57

Table 7.1. Mean and standard deviation of strain parameters of healthy controls and RhA patients 64

List of Figures

Figure 1.1. What is a strain? 9

Figure 1.2. Principle of 2D speckle tracking-derived strain 11

Figure 1.3. Longitudinal strain 14

Figure 1.4. Mathematical relationship between different strain parameters adapted from Thomas Binder et al. 14

Figure 1.5. The upper panel shows the strain rate curves of a middle-aged normal individual with systolic and diastolic strain rates shown. 20

Figure 2.1. Example of Tomtec analysis, right atrial speckle tracking evaluation 27

Figure 2.2. Example of ACP Toshiba. Right atrial speckle tracking algorithm. 27

Figure 2.3. Graphical representations of right atrial strain parameters 28

Figure 3.1. PALS inter-observer variability plot 31

Figure 3.2. PACS inter-observer variability plot 31

Figure 3.3. Booster pump (atrial kick) inter-observer variability 31

Figure 3.4. Reservoir phase SR variability 32

Figure 3.5. PALS intra-observer variability 33

Figure 3.6. PACS intra-observer variability 33

Figure 3.7. Booster pump intra-observer variability 33

Figure 3.8. Reservoir phase intra-observer variability 34

Figure 4.1. Histogram with normality curve of PALS, PACS, S`, E, A` 38

Figure 4.2. Q-Q plots of PALS, PACS, S, E, A 39

Figure 4.3. PACS and PALS as defined by Padelleti et al. 43

Figure 5.1. Bland–Altman plots of PALS and PACS, S` and E` between echo and CMR 48

Figure 6.1. Reproduced from Paulus et al: How to diagnose diastolic heart failure 53

Figure 6.2. Histogram with normality curve showing normal distribution of strain data 54

Figure 6.3. Q-Q Figure 6.4 Q-Q plots of PALS showing its normal distribution plot of PACS showing its normal distribution 55

Figure 6.4. Box plot showing the decreased conduit function of the right atrium in HFnEF patients as compared to normal controls. 56

Figure 6.5. Box plot showing decreased reservoir function of the right atrium in HFnEF patients as compared to normal controls. 56

Figure 7.1. The bar chart with normality curves for the S`, A`, booster pump and PALS: The curves show that data is normally distributed with major peaks in the centre of the the Gaussian distribution curve. 62

Figure 7.2. Q-Q plot of the strain and SR parameters 63

Figure 7.3. Strain difference between healthy controls and the Rheumatoid Arthritis patients 64

Acknowledgements

I would like thank my supervisors Prof. Paul Leeson and Prof. Stefan Neubauer whose constant guidance was instrumental at each step of my research. I have often lost sight of my goal and got distracted but their continued guidance and advice brought me back on track. They acted not just as my supervisors but also my life mentors as well. I would also like to pay tribute to my parents, sister and my in-laws whose prayers, advice and reassurance kept me going even in difficult times. My lovely wife and kids who inspired me to take one-step forward when the odds were pushing me to step back deserve my deep gratitude. I would also like to thank Dr Yasser Bhatti, Saba Riaz and their lovely family who provided a homelike environment in Oxford. Special thanks to Dr Daniel Augustine and Dr Merzaka Lazdam for helping and guiding me so much during my very early and fragile days at CCRF. A big thank you to Dr Sairia Dass, Dr Vanessa Ferreira, Dr Cameron Holloway, Dr Ntobeko Ntusi, Dr Erica, Dr Alex Pitcher, Dr Masliza, Dr Andrew Johnson and Dr Joe Suttee for being wonderful company in my brief but splendid stay at OCMR. Miss Jane Francis, Dr Theo and Dr Saul Myerson – you were great teachers. I would also like to thank Adam, Eduardo and Alex, who were by far the biggest source of inspiration and support for me. Special thanks to Esther for always being there for help and support. Thanks to James for listening to my ideas with patience. Polly, Yvonne, Kate, Rachel and Jonathan – you were the most wonderful people I have worked with so far. Thank you Barbara for reminding me every day that cleanliness is a good habit. Lastly, I would like to say a big thanks to my college advisor Dr Jonathan Reynolds, my College Fellows at Green Templeton College who have helped me in so many ways. The story is incomplete without mentioning my guru Dr Nikhil Pal and Dr Raja Jayaram, who were there to help at each step of my stay in

Oxford. I cannot thank enough my funding agency, higher education commission of Pakistan, as without their financial support the “Oxford Dream” would have never been materialized.

Chapter 1

Introduction

1.1 Location

The right atrium is located on the anterosuperior aspect of the heart, anterior and inferior to the left atrium.

1.2 Early History

William Harvey first described the right atrium in the 17th century. In Chapter 13 of his book "De Motu Cordis", Harvey wrote: "It has been shown by reason and experiment that blood from the beat of the ventricles flows through the lungs and heart and is pumped to the whole body. There it passes through pores in the flesh into the veins through which it returns from the periphery everywhere to the center, from the smaller veins into the larger ones, finally coming to the vena cava and the right atrium."

1.3 Anatomy

The right atrium has unique morphological and physiological characteristics, which differentiate it from the other cardiac chambers. The right atrium has four components identified by several landmarks:

1 The venous component, which forms the opening of the superior and inferior venae cavae and the coronary sinus.

2 The vestibule, which is a circular area at the margins of the tricuspid valve to which the cusps of the tricuspid valve are attached.

3 The right atrial appendage, which lies anterior to the crista terminalis, is on the lateral side of the right atrium and is composed of arrays of pectinate muscles.

4 The inter-atrial septum, which separates the atria and contains the fossa ovalis.

1.3.1 Histology

The inner surface of the right atrium has a network of longitudinally and radially arranged fibrous bundles called trabeculae.[1] The right atrial appendage, crista terminalis, and those overlays are formed from these bundles and are important landmarks because they contribute to the electrical properties of the right atrium and are therefore relevant to myocardial deformation.

1.3.2 Right Atrial Appendage

This is a small cavity located in the superior aspect of the right atrium. It has an arrangement of fibres that are much straighter than the rest of the atrium and the right ventricle, thus making it more distensible and more prone to fibrosis[2].

1.3.3 Crista Terminalis

The crista terminalis lies between the venous component and the right atrial appendage. It is a c-shaped fibrous-muscular ridge, which embeds in the right atrial wall. It has marked myocyte junction anisotropy, which is a substrate for micro-re-entry circuits; for example, a distinct entity called the "Cristal Atrial Re-Entry Tachycardia"[3] arises from the crista terminalis due to its unique structural and electrophysiological features. The crista terminalis can also act as an electrical barrier between the two territories that it separates. Its position is variable in the right atrium, hence leading to novel

electrophysiological phenomena.[4, 5] These electrical phenomenon differ in terms of the site of origin from the crista terminalis, thus, having different morphology and different refractory periods if they arise from upper end, mid portion or the lower end of the crista terminalis[3].These electrical phenomena in turn have the potential to affect the strain (deformation) of the right atrium.

1.3.4 Fossa Ovalis

The fossa ovalis is an embryological remnant of the septum primum and septum secundum. It closes in postnatal life leaving a mark-like impression called the foramen ovale. Sometimes it persists and is associated with risk of paradoxical embolism, stroke, and migraine.

1.3.5 Coronary Sinus

The coronary sinus is the venous drainage chamber of the myocardium, which opens into the right atrium, and the Eustachian valve guards its opening.

1.4 Right Atrial Physiology

The right atrial mechanics involve three main phases: a reservoir phase, the conduit phase, and a booster pump (the contractile phase). The right atrium acts as a reservoir during ventricular systole, a conduit during early diastole, and as a contractile pump during late ventricular diastole.

1.4.1 The Reservoir Phase

This phase of atrial dilation coincides with ventricular systole. After the closure of the tricuspid valve, blood from the superior and the inferior venae cavae and the coronary sinus enters the right atrium. The reservoir phase is synchronized with the QRS complex

and extends through the isovolumic contraction, ventricular systole, and isovolumic relaxation of the ventricle.

The right atrium stretches against the closed tricuspid valve due to its inherent distensibility while operating on the Frank–Starling mechanism.[6-9] The duration of the reservoir phase and the amplitude of dilatation reflect the potential energy stored in the atria. The reservoir phase provides four-fifths of the potential energy stored in the right atrium needed for effective atrial kick. The reservoir phase depends on the intrinsic compliance of the right atrium and the right atrial relaxation properties. Right ventricular base moves down during this phase to further facilitate this phase.

1.4.2 The Conduit Phase

This is the passive filling phase, which occurs during the early part of the ventricular diastole. During this phase, the ventricles fill "passively" without active energy expenditure by the atria. It starts from the opening of the tricuspid valves and ends just before the start of active contraction of the atria after the P wave on the ECG. This phase depends upon right atrial stiffening properties as stiff atria behaves as a different conduit than a compliant atrium. Moreover, right ventricular relaxation properties also affect this phase because if the right ventricular pressure is increased due to abnormal relaxation , it will offer more resistance to the entry of blood from the right atrium.

1.4.3 The Contractile Phase

The active pumping phase of the atria contributes about 15–30% of the stroke volume of the right ventricle. This pumping activity is lost in diseases like atrial fibrillation, where chaotic movement of the atria affects atrial contribution to the ventricles. The contractile phase depends on intrinsic contractility and is affected by right ventricle compliance.

1.5 Assessment Of Right Atrial Structure Through Imaging

1.5.1 History of Imaging of the Right Atrium

The invention of the echocardiogram, by Hertz and Igne Edler in 1951, opened the way for exploration of the heart. In 1965, Feigaunbaum *et al* did pioneering work on pericardial diseases through M-mode echocardiography, but the right atrium could not be explored because of the limited views of M-mode echocardiography. Boomer *et a*l were the first ones to describe the right atrial dimensions in 1979.[10] After that, there were a series of studies on the structure and functional aspects of this chamber, which are going on even now.

1.5.2 Echocardiography

Echocardiography is portable, radiation free, safe, easily available and is used in the study of the right atrium for the assessment of the atrial masses, pulmonary hypertension, tricuspid stenosis and regurgitation, congenital heart disease and atrial fibrillation. We can use it to investigate the relaxation properties and the diastolic phenomenon due to its high temporal resolution. However, it is operator dependent, is limited by anatomical views (even on trans-oesophageal echocardiography) and tissue characterisation is not possible as is possible in magnetic resonance imaging (MRI).

Keller *et al* used freehand drawing on 3D echocardiography and showed good correlations between 3D echocardiography and the MRI.[11] This study showed high variability at 124% on 1D and 37% variability on 2D echocardiography, while it is only 11% for 3D echocardiography and a bit higher for CMR. Schabelman et al compared 2D echocardiography to cineangiography in 1981.[12] A study by Koka *et al* showed that volumes measured by Multidetector CT are higher than those measured by 3D echocardiography.[13] Trans-oesophageal echocardiography has also been used for atrial

assessment. Spontaneous echo contrast on trans-oesophageal echocardiography has been linked to atrial thrombus formation.[14, 15]

1.5.3 Cardiac MRI

Cardiac MRI has an advantage over other modalities in terms of it being operator independent, having good tissue–blood contrast and being able to acquire extra anatomical planes. Late Gadolinium Enhancement (LGE) imaging is used for investigation of atrial fibrosis, atrial remodelling and left atrial appendage thrombi and stroke risk assessment. However, studies using MRI for the right atrium are relatively sparse. Akoum *et al* used LGE MRI to show that right atrial fibrosis correlates with sinus node dysfunction (SND).[16]

Ozgun *et al* showed that CMR is useful in studying right atrial volume and function and measuring cavotricuspid isthmus length, which is a predictor of atrial flutter.[17] Fleck *et al* studied right atrial function pre- and post-ablation, and showed that atrial contractility returns to normal after ablation.[18]

1.5.4 MDCT and cineangiography

Multi-Detector Computer Tomography (MDCT) is a robust technology for the structural and functional assessment of the heart. It has advantages like CMR in terms of being operator independent, offering the luxury of extra anatomical views and high spatial resolution. However, radiation exposure and contrast injection are its drawbacks.

The role of MDCT in the assessment of atrial septal defects has been explored in the recent past.[19] The right atrium has also been studied in cineangiography. A study by Carbera *et al* showed that the right atrium isthmus and the right atrium were significantly larger in patients with atrial flutter than controls.[20]

1.6 Assessment Of Right Atrial Function Through Imaging

1.6.1 Conventional Echocardiographic Measures

There are several measures of atrial function in "traditional" echocardiography, with some limitations. The commonest measure used is tricuspid inflow velocities and velocity time Integral of A wave of tricuspid inflow velocities. However, it measures the contractile force of the atria and flow from atria and is highly dependent on the loading conditions of the heart and diastolic function of the ventricle. Tissue Doppler-based atrial velocities and the velocity time integral are measures used but they have limitations in terms of being angle dependent and needing high frame rates for good image resolution. Atrial ejection force is a measure of atrial systole commonly used but again this is dependent on the loading conditions of the heart. Similarly, the atrial emptying fraction is also used to measure atrial function, instead of ejection fraction, since it is mostly the emptying of the atria rather than ejection. Atrial phasic volumes have shown to be important in diagnosis and prognosis of Pulmonary Hypertension and other pathologies but are load-dependent.

1.6.2 Novel Techniques to Assess the Right Atrial Function

Cardiac function is traditionally measured with trans-thoracic echocardiography via volumetric measures of cavity size (end diastolic volume and end systolic volume[21]), mass[22] and ejection fraction.[21] Although they are well-validated parameters and have diagnostic and prognostic significance, ejection fraction and volume are load dependent.[23] Ejection fraction varies when the heart lengthens or shortens. Additionally, ejection fraction (the most commonly used measure in clinical practice) cannot differentiate prognostically between heart failure with preserved ejection fraction (HFpEF) and heart failure with reduced ejection fraction[24]. Moreover, volume, mass and

ejection fraction give an estimate of global myocardial function with no or very little information about the regional function of the myocardium.

Myocardial function depends mainly on three factors: 1) preload; 2) after load; and 3) contractility. While we can measure loading conditions with reasonable accuracy, the measurement of contractility is fraught with many technical difficulties and challenges. The most notable of these is its dependence on loading conditions and inotropic state. There are several indirect measures of contractility such as cardiac output, stroke volume, end diastolic and systolic volumes and ejection fraction but they all have the same technical limitation as mentioned above.[25] For accurate measurement of contractility, we need to have a measure which is at least relatively independent of the loading conditions of the heart and which measures the deformation and motion of tissue micro-architecture, or in other words which is a true representative of tissue signal.

Strain is a measure introduced relatively recently in the cardiac community, which, if considered in one dimension, is due to a change in the length of a one-dimensional object relative to its original length. It is described by the following formula:[26]

$$E = \frac{L - L_0}{L_0}$$

Lo is the original length and L is the final length.

Unfortunately, no such ideal measure is widely available. However, myocardial strain as measured by speckle tracking echocardiography (STE) is a relatively load-independent measure of myocardial contractility.

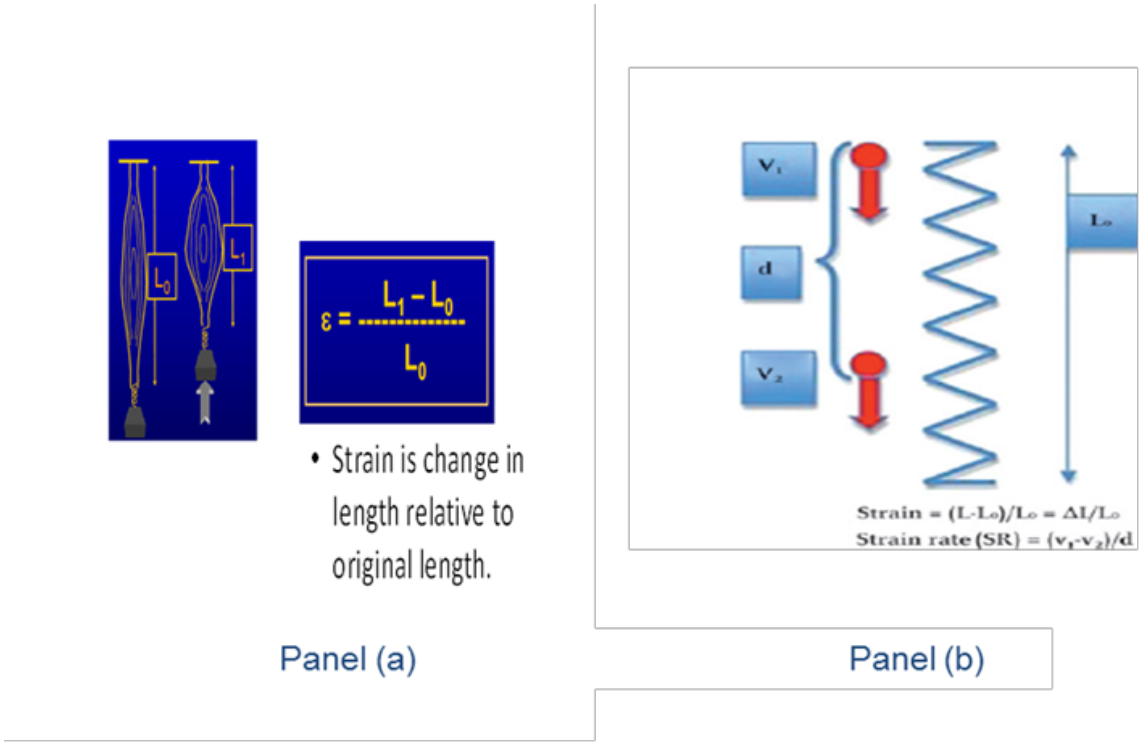


Figure 1.1. What is a strain? Panel **a**: Strain is defined as the deformation of an object, normalized to its original shape. Panel **b**: Strain Rate (SR) should be understood as the rate of myocardial deformation over a period of time.

Several methods of measurement of strain have been reported in the experimental literature but myocardial strain is principally measured through tissue Doppler methods[26, 27] and more recently developed STE.[28-33] Doppler-derived strain is a robust, easily available, reproducible technique. However, for accurate data recording it requires a high frame rate (100–150 frames/second (FPS)) and is angle dependent[34] as well as being affected by translational movements and tethering and algorithms are computationally complex.

1.7 Speckle Tracking Echocardiography (STE)

1.7.1 Principles of Speckle Tracking

STE is an innovative technique with huge potential for transforming cardiology practice. It is robust, reproducible, accurate, and free of angle of insonation problems. Moreover, the frame rate requirement is not as high (60–90 FPS). STE has been shown

to have good inter-observer and intra-observer variability.[28] STE has been validated against sonicometry and CMR.[28, 35] It tracks tissue "signatures" or ultrasound image texture formed by attenuation, reflection, and refraction of sound waves from myocardium. When sound waves meet the human body, they get scattered by the ribs, lungs, myocardium, air tissue interfaces, and the blood. Some of the sound waves are attenuated by losing their intensity while penetrating the tissues. The waves, which are scattered, are in decoherent form, which means that the crest of one falls over the trough of the other at some places and vice versa. At some places they cohere (add up) while at others they decohere, (nullify each other). Despite this coherence and decoherence there are some waves of very small wavelength that are smaller than the resolution of the imaging system. They form the "noise" in the imaging process. When subsequent processing steps are applied, these noisy waves have a mottled appearance and this is what has been called the "speckle pattern." These speckles are assigned a functional unit called a "kernel," which is then used in tracking the myocardium throughout the cardiac cycle.

The other half of the picture – "tracking" or spatial dislocation[36] – is even more interesting. These "speckles" can be used to track the movement of the underlying myocardium from which they originated. Since these speckles are formed from sub-resolution wavelength waves, they represent fine fingerprints of underlying myocardial. Complex algorithms can be applied to track these speckles. Although the scope of these algorithms is beyond this document, in essence the statistical methods used are similar to block matching and autocorrelation techniques[37, 38].

1.7.2 Speckle Tissue Architecture or Random Noise

Much of the property of echocardiography (ultrasonic images) depends on the texture of the image. The study of the texture of the image remained an area of active research for quite some time. Whether this grainy texture "speckle" is a tissue signal or just random noise has been a matter of great debate. While some research groups applying stochastic (random) analysis successfully predicted the course of these speckles,[39] others had success in associating tissue microstructure with the speckle pattern. However, some of these experiments[39] showed that when ultrasound properties remain the same the speckle pattern is the same, while when ultrasound transducer settings are changed the speckle pattern is different from the former pattern. Additionally, the size of the speckle granule has been shown to be proportional to the resolution of the ultrasound scanner. More recently, it has been shown that we get a specific micro-architecture even on near infinite magnification on optical imaging techniques (optical microscopy, for example). The ultrasonic or echo speckle pattern no longer represents the tissue architecture, even on a few orders of magnification.

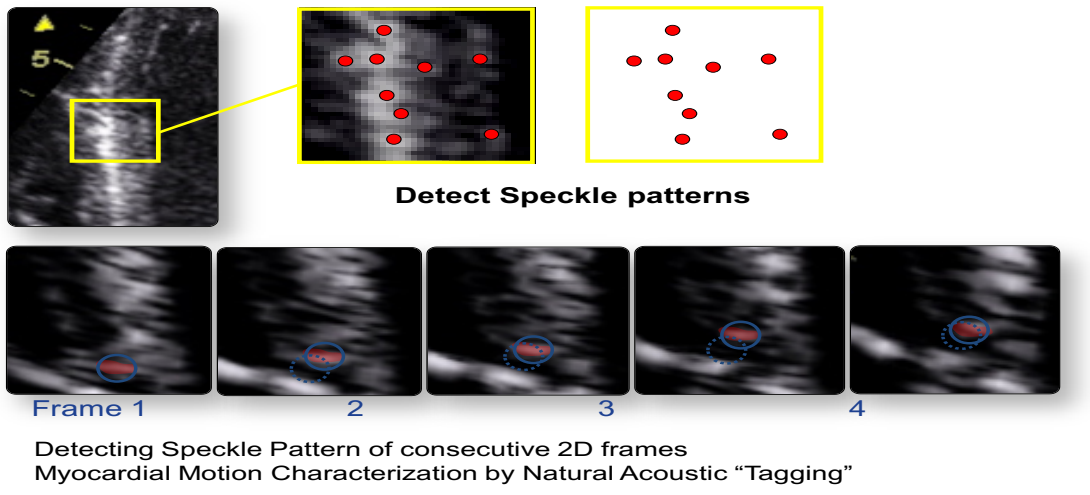


Figure 1.2. Principle of 2D speckle tracking-derived strain

1.7.3 Strain Parameters Derived from STE

STE measures the parameters of deformation (change of shape), namely strain and SR, and parameters of motion (velocity and displacement). When one part of an object moves while other parts remain constant, there is a change in shape (deformation) in the object, while when both parts move there is movement of the object (motion). Since the heart is a three-dimensional structure it can lengthen and shorten along its long axis, contract along its circumference, thicken, and thin along its radius. Therefore, we have longitudinal strain, radial strain and circumferential strain.

Longitudinal Strain:- Longitudinal strain is a measure of movement of the heart segments along its long axis. According to the architecture of the myocardial fibers, the longitudinal fibers are arranged spiralling outward in longitudinal direction, middle layer is arranged circumferentially and epicardium fibers spiral inward direction. Endocardial fibers contribute to longitudinal strain. This has been proven in experimental studies where decrease in longitudinal strain is predominant abnormality in sub-Endocardial Myocardial Infarctions.[36] Longitudinal strain is measure in apical 4 chamber, 2 chamber and 3 chamber views. The mechanism underlying longitudinal strain is active contraction of base of the heart relative to the apex, which results in generation of pressures to eject the blood from left ventricle to the aorta. In normal individuals, left ventricular lateral wall contracts more than septum.

Circumferential Strain:-The middle layer of the left ventricle is arranged in circumferentially arranged fibers and is responsible for circumferential strain. It is measured in short axis views.[40]

Radial Strain:- Radial strain is not a very robust and reproducible measure of ventricular function but most algorithms still use it. The epicardium contributes 7% of the

myocardial layer, and the endocarpdium 56%. Hence, it is not affected in subendocardial infarcts but affected in trans mural infarcts.

Strain Rate: - Strain Rate is the rate of change of strain and it is the temporal derivative of strain and unlike strain, which is a measure of systolic function mainly, it is a better measure of diastolic phenomenon. Expressed as (1/s).

Twist and Torsion: - The apex and base of the heart rotate in opposite directions leading to writhing movement of the heart, which accounts for 15-30% of the ejection fraction. This clockwise and counterclockwise motion of the apex and base are measured in degrees and is called Rotation. Twist is the difference between base and apex rotations. Twist and torsion have been used alternatively in literature but there is growing consensus that torsion is the twist rate given by dividing the twist on the length of the chamber. [41-44]

Table 1.1. Strain Parameters

Variable	Description
Strain	Change in length relative to original length (L-Lo/Lo)
Strain rate	Rate of change of strain or change in strain over time showing systolic and diastolic phenomenon
Longitudinal Strain	Strain along the long axis of the left ventricle.
Radial Strain	Thickening or thinning of myocardium
Circumferential strain	Strain along the circumference of left ventricle
Rotation	Direction of movement of base or apex of the heart
Twist	Difference in rotation of apex and base of the heart
Torsion	Twist divided by length of left ventricle



Figure 1.3. Longitudinal Strain

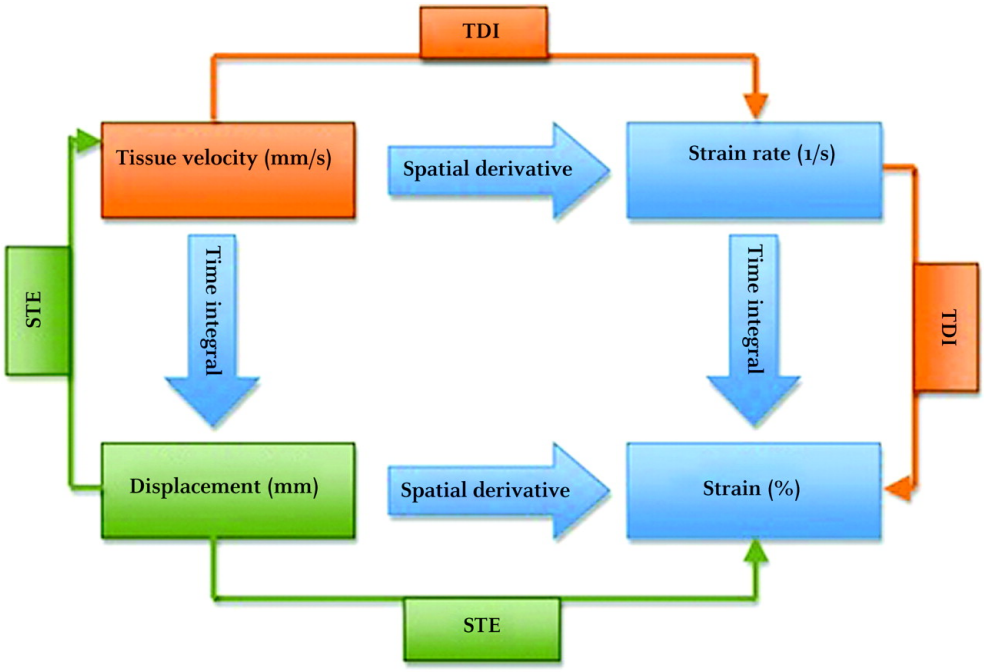


Figure 1.4. Mathematical relationship between different strain parameters adapted from Thomas Binder et al. [40]

1.7.4 Image Analysis

On most custom software (e.g. ACP Advance Toshiba Medical; Tomtec, Germany; Qlab, Philips; Echopac, General Electronics) we get the curves of global and segmental values of strain, SR, velocity and displacement. From the left ventricle we record

systolic and diastolic values for SR and velocity while the systolic values of strain and displacement are measured. The strain should be calculated from at least three consecutive heartbeats. Vendor dependent and independent software have shown good agreement for longitudinal and circumferential strain, while radial strain measurements are less reproducible than longitudinal strain [45, 46].

Left ventricular longitudinal strain is measured from apical four chambers, apical two chambers, and sometimes using a three-chamber view. Longitudinal strain is the motion from base to apex. During systole, the left ventricle shortens from base to apex; hence, a negative value for deformation is generated. Radial strain and circumferential strain are measured from a mid-ventricular short axis view. The twist is the difference in rotation (measured in degrees or radians) of the left ventricle between apex and base. Torsion denotes the twist divided by the distance between the apex and base.

1.8 Applications of STE

1.8.1 Hypertension

Hypertensive patients with left ventricular hypertrophy have relaxation abnormalities which are manifested as a decreased untwisting and untwist rate in STE.[47] In hypertensive subjects with NYHA Class 1 heart failure, the basal longitudinal strain (an indicator of the longitudinal function of the base of the heart) is reduced. Patients with NYHA Class 2 have basal and mid-longitudinal reduced strain, while longitudinal strain is reduced globally in NYHA classes 3 and 4. Radial and circumferential strain are also reduced in more pronounced heart failure.[48]

1.8.2 Diabetes

In addition to its role in cardiac diseases, STE appears to have a role to play in metabolic disease as well, the most notable contribution being diabetes. Speckle tracking echocardiography has shown that in young patients with Type 1 diabetes, the early untwisting rate (E) (the early part of diastolic filling) is preserved while the late untwisting rate (A) (the atrial contribution to left ventricular diastolic filling) is decreased.[44] In Type 2 diabetes, the systolic dysfunction as detected by STE is one of the earliest markers of diabetic cardiomyopathy. The decrease in systolic function is mainly due to decreases in longitudinal and radial strain, even after adjustment for age, gender, and blood pressure.[49] However, another study reported impairment of the longitudinal systolic and diastolic function but preserved radial and circumferential function in patients with Type 2 diabetes.[50] The decrease in longitudinal strain was associated with the duration of diabetes. Moreover, LV torsion (which creates the suction pressure during diastole important for ventricular filling and hence ventricular contractility) tends to increase in Type 1 asymptomatic patients as compared to healthy controls, which might be a compensatory factor to offset the decreased longitudinal and radial strain. Longitudinal fibres are most sensitive to ischemia and hence the longitudinal strain as evidenced by TDI and STE tends to increase first before decreasing[51, 52]. Later on, torsion is the compensatory mechanism to account for the salvaging of myocardium. Torsion is independent of micro vascular obstruction as shown by the negative correlation with the stress fusion index or MPRI.[53, 54]

1.8.3 Hypertrophic Cardiomyopathy

Hypertrophic Cardiomyopathy (HCM) results from myocardial disarray due to genetic causes and, in echocardiography, differences in mitral valve function as well as diastolic

dysfunction can be identified. There is also systolic dysfunction, which is difficult to characterise by routine echocardiography.[55] STE has proven to be a useful diagnostic modality for elucidation of systolic abnormalities in HCM patients. Longitudinal, radial, and circumferential strains are decreased in STE in patients with HCM. On segmental analysis, basal segmental strain is reduced more than other segments.[56] Left atrial longitudinal functional is decreased in HCM, which can be studied through STE.[57] Notomi et al[43] showed that the untwisting rate is impaired in HCM as compared to normal subjects. Patients with HCM have decreased LV and LA longitudinal strain and high LA volumes, which can also be detected using STE.[58] Furthermore, STE has been used to show dysfunction of the RV in addition to LV and LA.[59]

1.8.4 Dilated Cardiomyopathy

The left ventricular apex rotates counter clockwise during systole and the base rotates clockwise, while during diastole untwisting takes place. The myocardial protein titin acts as an elastic molecular spring to facilitate this uncoiling process and is thought to be important in the development of dilated cardiomyopathy. This untwisting process is important in diastole as it creates a suction pressure during diastole. The velocity of untwisting decreases in non-ischemic dilated cardiomyopathy, showing that the link between systole and diastole is impaired in DCM.[60] STE may have a role in determining the need for Cardiac Resynchronisation Therapy (CRT) in patients with idiopathic dilated cardiomyopathy, as the LV rotation and dispersion indices are decreased in DM patients and improve significantly after CRT.[61]

1.8.5 Restrictive Cardiomyopathy (RM) Vs. Constrictive Pericarditis (CP)

STE may be useful to differentiate CP from RM. In RM, the longitudinal strain is decreased while in constrictive pericarditis circumferential strain is primarily reduced.

Moreover, early diastolic recoil is decreased in each of the relevant directions in the two conditions.[62]

1.8.6 Inflammatory Cardiomyopathies

The radial and longitudinal global and segmental strain has been shown to be decreased in RhA patients even in the absence of cardiovascular disease or risk factors and otherwise normal echocardiography parameters.[63] It has been shown that LV end systolic longitudinal and radial strain has been decreased in RhA patients despite normal echocardiographic parameters[63]. Another recent study showed decreased RV and LV global longitudinal function in RhA patients as compared to healthy controls and the deformation parameters correlated well with the disease severity[64].

According to another study, RhA patients have decreased sub clinical strain parameters which are associated with nitro-oxidative stress and decreased endothelial function, this function improves by administration of Anakinra, a drug which selectively blocks IL-1 function[65].

1.8.7 Takutsubo Cardiomyopathy

STE has been used to elucidate the pathophysiology of this relatively common but under-diagnosed disease (Stress Induced Cardiomyopathy). During the acute phase of the disease the systolic dysfunction has been found to be predominantly in the circumferential and radial directions, which is different from the dysfunction seen with coronary artery disease, while, during the late phase the dysfunction resembles that seen in coronary artery disease.[66]

1.8.8 Valvular Heart Disease

Cardiac mechanics have been studied through STE in aortic stenosis (AS), aortic incompetence (AI) and mitral regurgitation (MR). In AS, contractility is reduced, which results in decreased exercise performance. Longitudinal strain is the first one to get affected in otherwise "normal" individuals.[67] LV RS and CS strain improve significantly after aortic valve replacement surgery, hence showing their load dependence.[68] Adda et al showed that longitudinal strain is one of the earliest parameters to get deranged in Low Flow Low Gradient (LFLG) AS.[46] STE has prognostic value as well in AS.[69] In chronic AI, the deformation indices pick up an early systolic and diastolic dysfunction and longitudinal strain is a sensitive marker of cardiac dysfunction in AI.[70] Left ventricular untwisting velocity and time to untwist (indicating the delayed suction phenomenon) are seen in patients with MR. On a broader level, this shows LV remodelling and LV diastolic failure due to hemodynamic changes occurring over time in MR.[71]

1.8.9 Miscellaneous

Speckle tracking echocardiography has been widely used in the detection of the extent of myocardial involvement in other metabolic conditions such as lipidosis[72] and hyperthyroidism.[73] Similarly, it has also been used to predict recovery from cardiothoracic surgery,[70] as an endpoint in clinical trials, and to study congenital heart disease.[74] STE has also been applied in dyssynchrony[75, 76] imaging, e.g. decision making for CRT selection and choosing responders vs. non-responders. STE can also determine the recovery post cardiac transplant.[77]

1.8.10 Emerging Applications

The applications of speckle tracking imaging are not limited to the left ventricle and it has been used for assessment of the right ventricle[78] (Figure 5), the left atrium[79-83] and right atrium.[84-86] In electrophysiology, high temporal resolution has led to its use for imaging activation of the atria as well as simultaneous electrical and mechanical imaging. Some of the future directions for the technique include new smart acquisition algorithms with more limited operator dependence. Some progress in this regard has been made and these algorithms would overcome the issue of operational problems in interpretation of image quality. Furthermore, it has also been proposed that speckle imaging could be used to assess the carotid vessels or the aorta. The concept of ultrasound speckle tracking is not limited to the heart as any structure with inherent ultrasound speckle can be assessed. STE has also shown promise for early and mid term follow up of after TAVI for hemodynamic changes and LV reverse remodelling.[87]

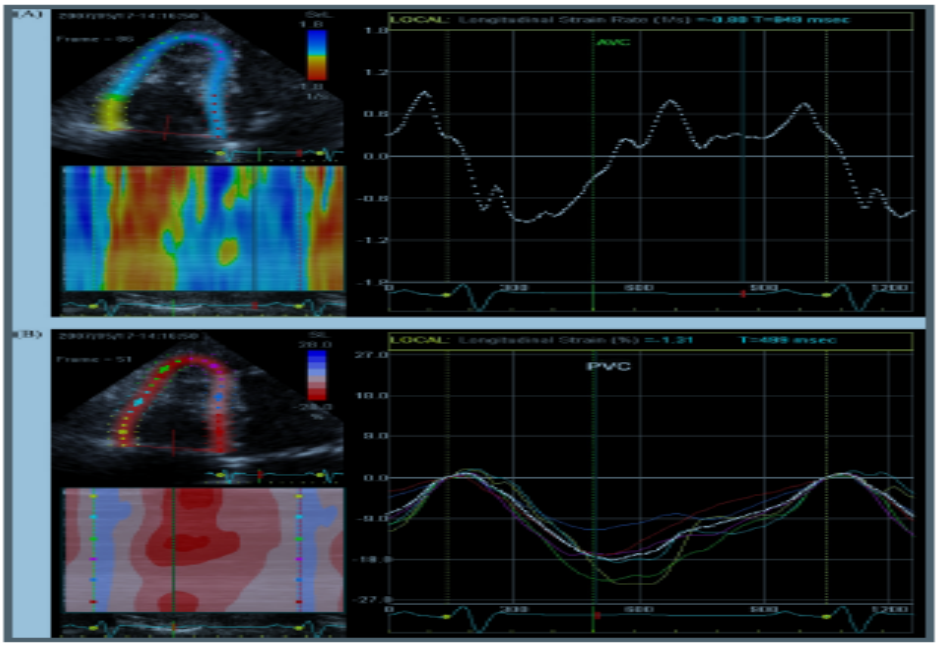


Figure 1.5. The upper panel shows the strain rate curves of a middle-aged normal individual with systolic and diastolic strain rates shown. While the lower panel shows the Strain curves for the right ventricle in the same individual showing regional (coloured lines) and global (white line))

1.9 Aim of Research

It is obvious from the above account that STE is a valuable tool, which has been extensively used for the LV, LA, and RV chambers. However, its use in the right atrial evaluation is very limited. The right atrium is important because of its unique mechanism, electrophysiological, and neuroendocrine properties, which influence its phasic strain. Before using a technique for a relatively unexplored chamber, we need to optimise and validate it so that there is accuracy of the reported results and the extent of variability can be judged.

Moreover, in order to compare the strain values with abnormal cohorts, the normal reference ranges should be defined. HFNEF is a unique cohort in which The left atrium has been shown to influence the pathophysiology and the prognosis. It is worth studying the role of the right atrium in the pathophysiology of heart failure with normal ejection fraction (HFNEF). Lastly, RhA is a unique disease in which right heart involvement secondary to pulmonary hypertension and due to cardiac fibrosis, itself have been reported.

This theis therefore tests the hypothesis that:

Right atrial deformation analysis can be performed using speckle tracking echocardiography and differs between healthy and diseased groups.

The aims of this study are as follows:

- To optimize speckle tracking echocardiography analysis technique for the right atrium (Chapter 2);
- Assess reproducibility of the technique for the right atrium (Chapter 3);
- To define normal reference ranges for right atrial strain (Chapter 4);

- Comparison of right atrial strain measured by STE and Feature Tracking CMR (Chapter 5);
- To study right atrial strain values in patients with HFnEF (Chapter 6);
- To study right atrial strain values in various inflammatory cardiomyopathies (Chapter 7).

Chapter 2

Methods of Image Acquisition and Analysis

2.1 Introduction

Standard methods have been developed to apply STE for the assessment of the left ventricle[60, 71, 88], the right ventricle and left atrium[89, 90] in health[79, 91-93 36, 94]and disease.[69, 71, 75, 95-97] Mechanical functional assessment of the right atrium remains less explored and a standardised STE technique for the study of the right atrium remains less well developed. In the current study, we standardised speckle tracking for the right atrium based on adaptation of left ventricular protocols.

2.2 System Settings

System settings for image acquisitions, transfer, and analysis were as follows:

- Echocardiography was performed using a Toshiba Artida echocardiography system (Toshiba, Netherlands) or a Philips ie33 (Philips Medical system, Netherlands).
- Echocardiography was performed on an echocardiography system equipped with a 2.5-3.5 MHz transducer with ECG gating in slight breath-hold in end expiration by trained echocardiographers (ML, DA, EL, ED, NP).
- Grey scale (B-Mode) 2D images were acquired for the analysis.
- Mechanical index was set at one. Frequency varied between 2.8 and 3.6 GHz.
- Second harmonic imaging was turned on for acquisition.

- Frame rate of 60–90 FPS was used as advised for optimal working of this algorithm to get good quality analysable images. 30 FPS was the lowest limit of the frame rate. Below that frame rate, speckles were unstable and above 120–150 FPS speckles decohere and hence the interference pattern is not the true representation of the actual image.
- An apical four-chamber view was acquired.
- Data were stored digitally remotely and analysed offline using an Advanced Cardiac Package Toshiba (ACP, Toshiba) and TomTec (Germany) on dedicated computers. The algorithm[98] designed by Reisner et al and used by others[30] was used in the analysis. All the data were analyzed on TomTec as it is a vendor independent software. However the data on the RhA study was in addition analyzed on ACP,Toshiba as images were acquired using Toshiba ultrasound machine.

2.3 Image Analysis

2.3.1 ACP Toshiba

ACP Toshiba allows an average of Toshiba image datasets by a standalone analysis package. The images are uploaded from disk or external hard drive and then undergo standard processes.

By default, the first 30% of the diastole were selected by the software. For atrial tracking, automated contouring was turned off because of the absence of a right atrial model for segmentation in the algorithm. The fixed thickness was selected to have the same thickness of endocardium in all segments. This tracking algorithm does not require a minimal wall thickness to track different layers. The right atrial appendage was excluded from the analysis by drawing a straight line across its orifice. The user manually places several small kernel regions (10–50 pixels in size), then (depending on

image resolution) along the Endocardial and epicardial borders on the end diastolic imagery, tracing the image series in an anticlockwise direction. The program then automatically places additional kernels at mid-distance between the Endocardial and epicardial borders and tracks the three borders (endo-, mid-, and epi-) on a frame-by-frame basis by use of a least-squares global affine transformation. Both global and segmental values on a six-segment model are generated. However, the segment representing fossa ovalis was excluded from the analysis due to poor tracking and very thin inter-atrial septum. The algorithm was run during the reservoir phase (maximum dilatation of the atria and ventricular systole).

2.3.2 Tomtec

Tomtec (Diogenes Medical, Germany) is vendor-independent software which can accept and analyze images from any echocardiography platform. The digitally stored data was uploaded to the Tomtec server. The user then selected the appropriate study and the image and program was initiated. On the user interface options, there are options for selecting a suitable view, adjusting the grey level and making the endocardial borders visible. The user can also select to manually contour the endocardium or draw it in a semi-automated fashion. Unlike Toshiba ACP, any phase of the cardiac cycle can be selected. For the purpose of our study, we selected the point where atria were fully expanded and the Endocardial border was fully visible. The endocardium and epicardium were traced by placing small dots (kernels) on the lining. Then the algorithm was run, which gave the visual map of strain, SR, velocity, and displacement. Volume curves were also calculated but were not used in our analysis. Regional and global strain with time-to-peak information was calculated in the next step. The segment representing fossa ovalis was excluded from the analysis due to poor tracking and thin walls.

2.4 Output

The generated values for strain, SR, velocity and displacement can be used for assessment of atrial mechanics. The first peak, during passive expansion of the right atrium against the closed valve, was reported as Peak Atrial Longitudinal Strain (PALS) (see Figure 5 below). The second peak during which the atrium acts as the conduit was reported as Peak Atrial Conduit Strain (PACS). Time to peak for both these events T2PALS and T2PACS was also reported.[84] The booster pump phase of the atrium during which atria actually contract was reported as the peak negative value. PALS can be used to represent the reservoir function, PACS was representative of the conduit function and atrial kick was represented by the booster pump function. For SR, the first positive value was labelled as "S" after the ventricular systole. The first negative wave was labelled as "E" and the second negative wave was labelled as "A". The E wave was used to measure conduit function and the A wave to assess contractile function. PALS corresponded in timing with S, PACS with E, and booster pump with A. An additional first positive velocity can be used to measure atrial fractional relaxation[99].

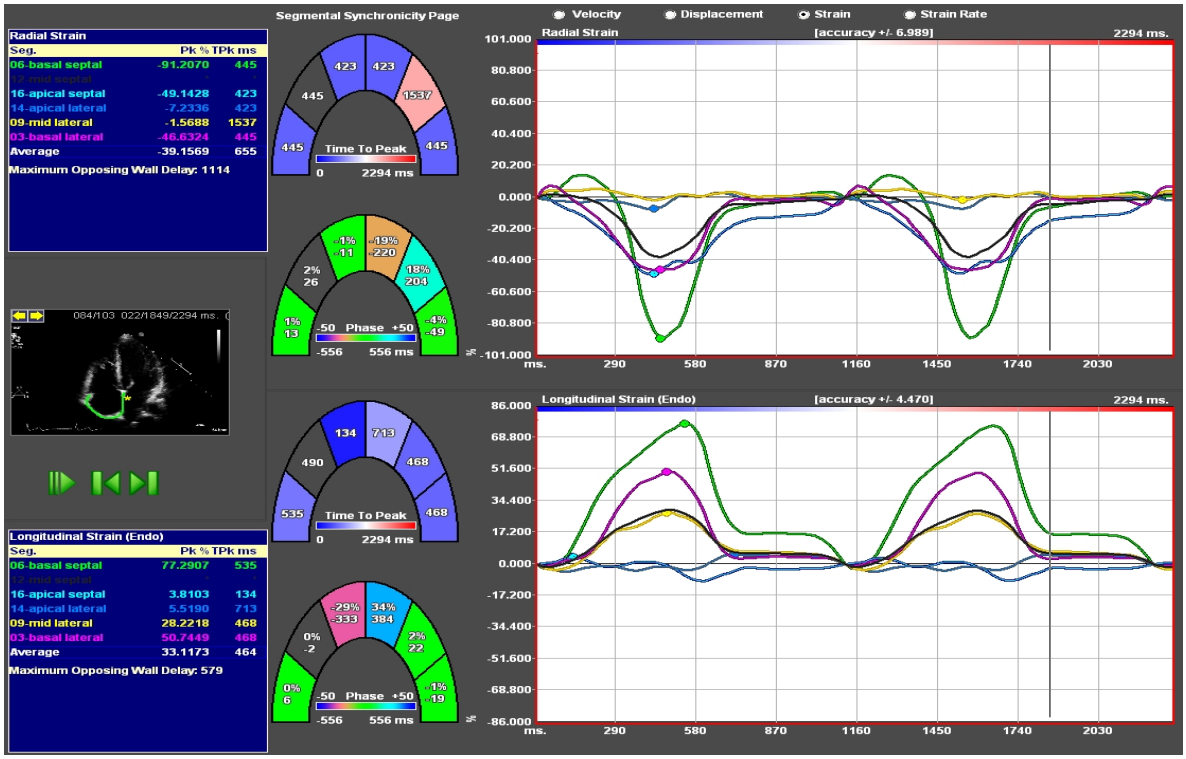


Figure 2.1. Example of Tomtec analysis, right atrial speckle tracking evaluation. Right atrial strain is reproduced, and PALS, PACS, the reservoir and the contraction phase, are measured.

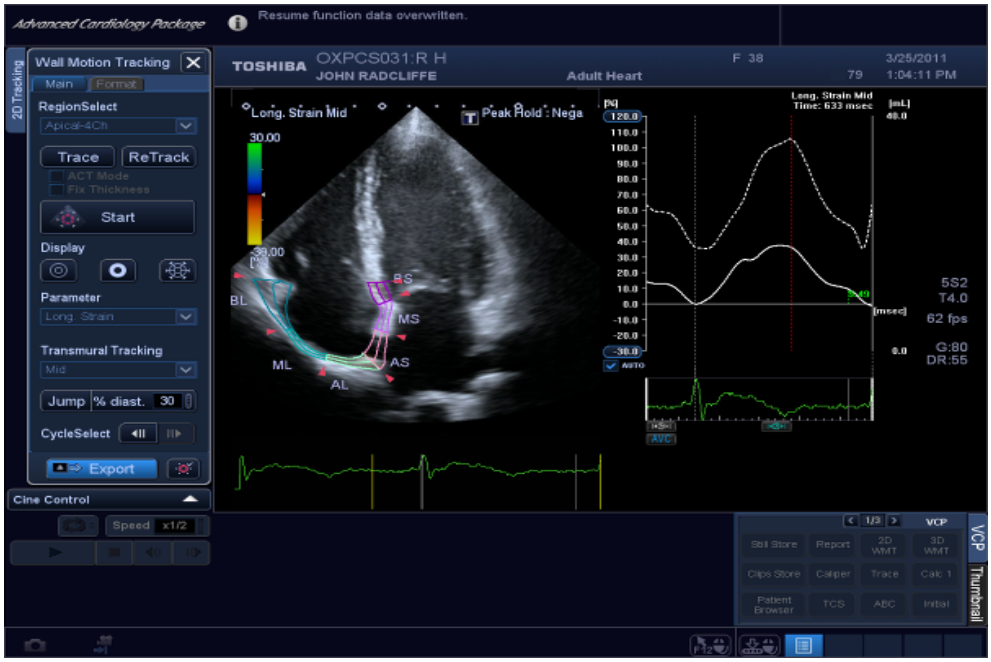


Figure 2.2. Example of ACP Toshiba. Right atrial speckle tracking algorithm. The right atrium has been divided into six segments. The top right curve is the volume-time curve and the curve below it the strain-time curve.

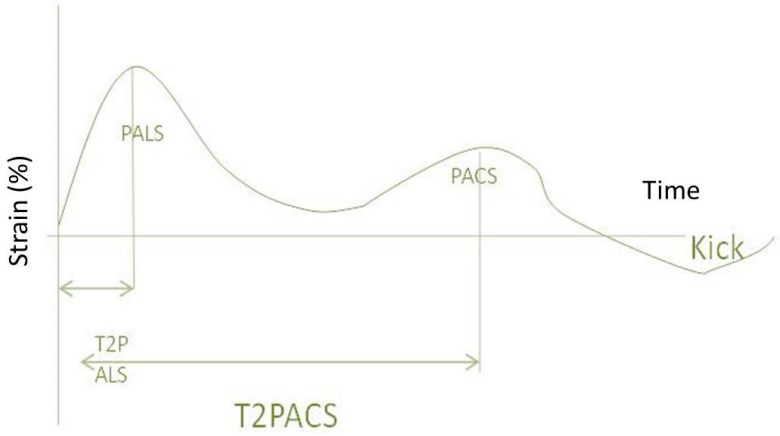


Figure 2.3. Graphical representations of right atrial strain parameters

Chapter 3

Reproducibility Study for Speckle Tracking-derived Right Atrial Strain

3.1 Introduction

Assessment of the left ventricle, right ventricle, and left atrium has been done through STE. However, very limited data is available on the reproducibility of speckle tracking-derived strain for the right atrium.[84]

Therefore, the aim of this study was to determine the reproducibility of the speckle tracking-derived strain for the right atrium.

3.2 Methods

3.2.1 Study Population

Eight patients in sinus rhythm, free of any form of cardiovascular, renal, hepatic, or respiratory disease were recruited as part of various ongoing trials. The local ethics committee granted ethical approval.

3.2.2 Study Procedure

Two persons (ABS and EL), both of whom have more than three years of experience in echocardiographic image analysis, repeated analysis separately in a blinded fashion. ABS also analysed all the images twice, a week apart.

3.2.3 Statistical Analysis

Tests of normality were done on the data. Normally distributed data were expressed as a mean (SD) while non-normally distributed data were distributed as a median and inter-quartile range. Bland–Altman plots were drawn to determine the inter-observer and intra-observer agreement and bias and limits of agreements were calculated.

3.3 Results

3.3.1 Interobserver Agreement

The interobserver limits of agreement and bias are given in Table 3.1, while the following figures show Bland Altman plots. It is obvious from the table that the limits of agreement are poor for the strains of all three phases of atrial physiology. In these tables and figure, strain rate for reservoir phase is given only because the curves for strain rate of conduit phase and atrial kick were not always very smooth and it was difficult to choose the exact point from where the values can be recorded.

Table 3.1. Inter-observer agreement for atrial phasic mechanics through Bland–Altman method.

Parameter	Limits of Agreement	Bias
PALS	-24.9-33.0	4.0
PACS	-27.0-13.4	-6.8
Booster pump	-3.2-8.8	2.8
S`	-0.87-1.54	0.33

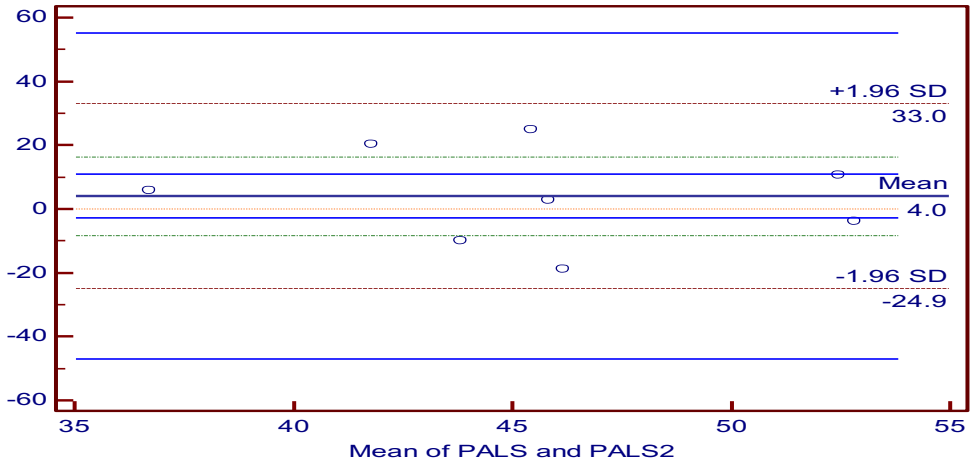


Figure 3.1. PALS Inter-observer Variability Plot

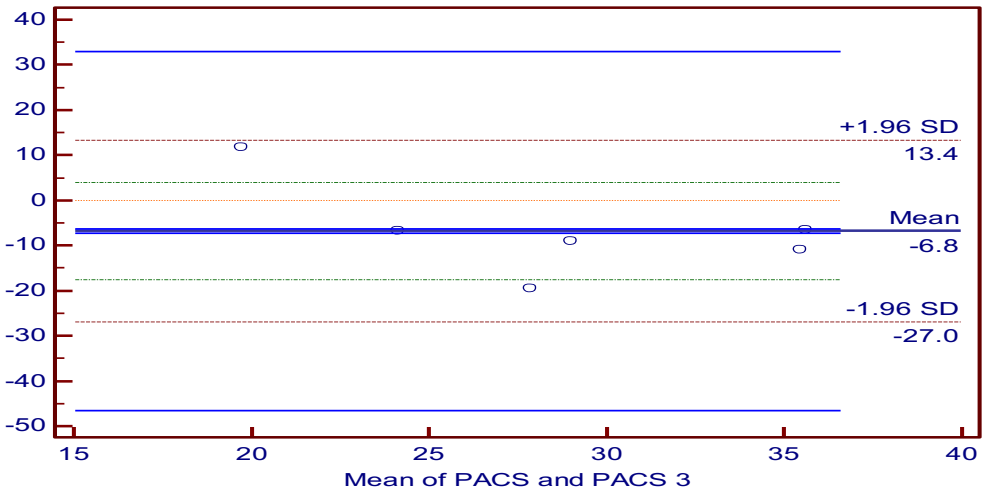


Figure 3.2. PACS Inter-observer Variability Plot

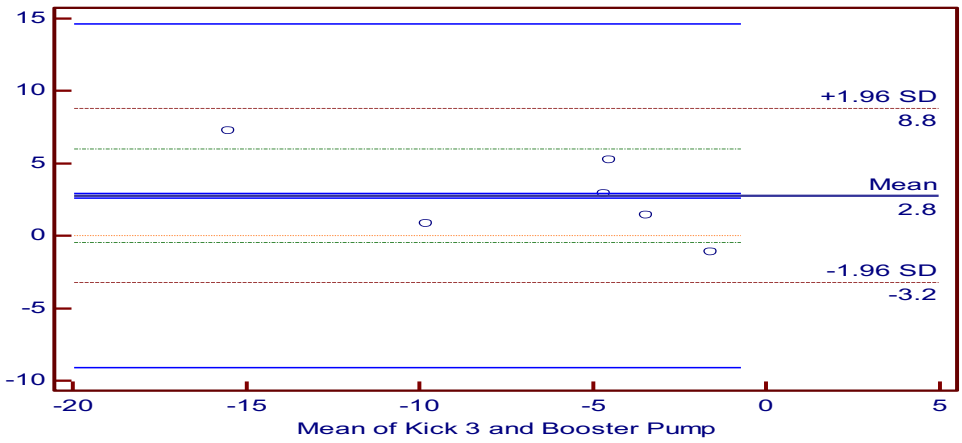


Figure 3.3. Booster Pump (atrial kick) Inter-observer Variability

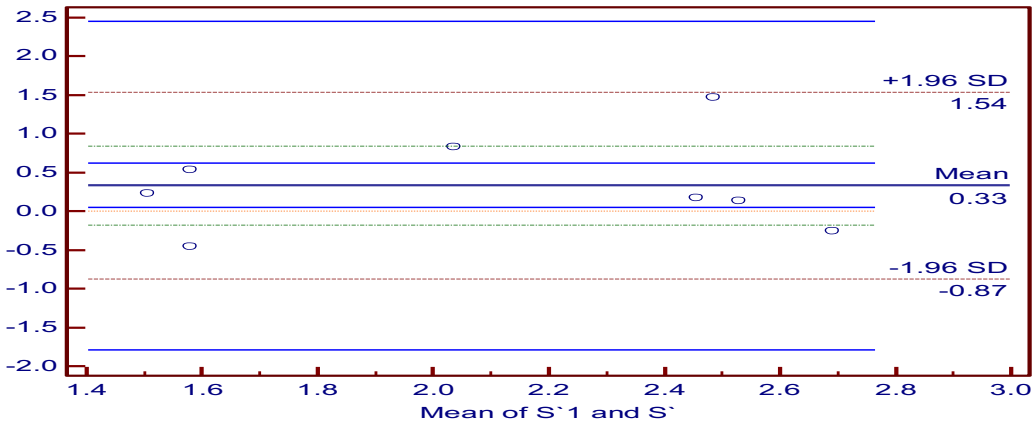


Figure 3.4. Reservoir Phase SR Variability

3.3.2 Intraobserver Agreement

Intra-observer limits of agreement and bias are given in Table 3.2, while the following figures show the Bland–Altman plots.

Table 3.2. The intra-observer limits of agreement and bias for right atrial strain

Parameter	Limits of agreement	Bias
PALS	-37.9-21.8	-8.1
PACS	--27.0-13.4	-6.8
Booster pump	--11.3-4.1	-3.6
S`	-1.2- 1.1	0.0

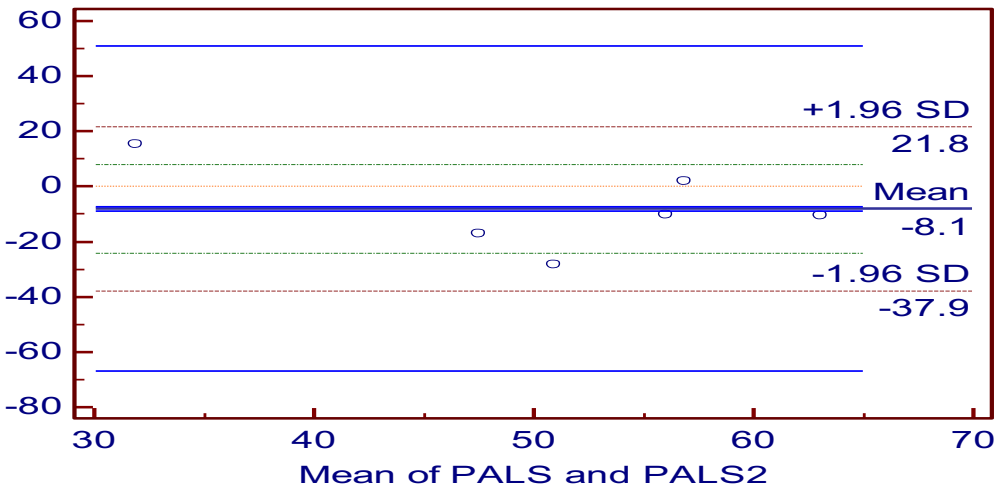


Figure 3.5. PALS Intra-observer Variability

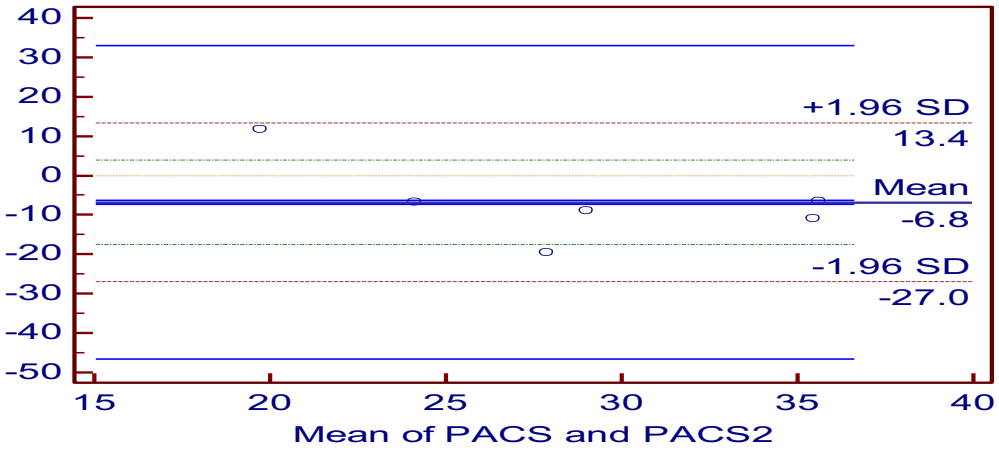


Figure 3.6. PACS Intra-observer Variability

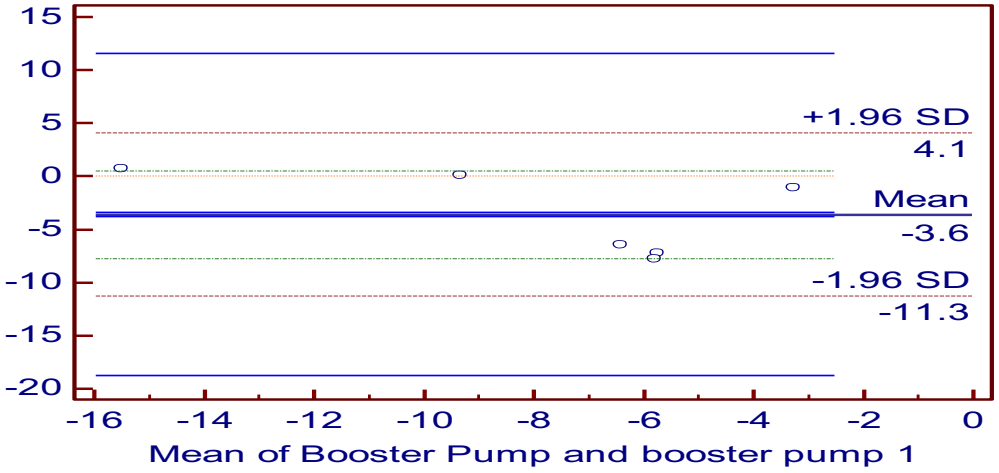


Figure 3.7. Booster Pump Intra-observer Variability

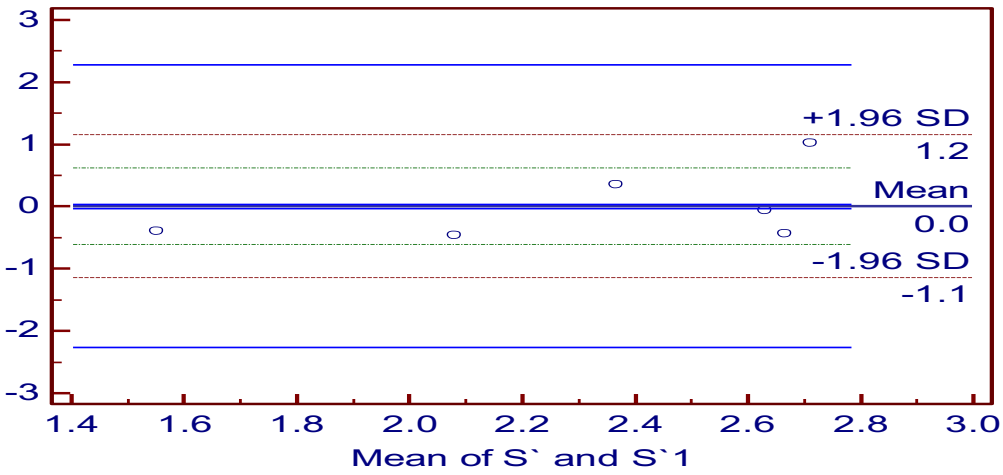


Figure 3.8. Reservoir Phase Intra-observer Variability

3.4 Discussion

This study demonstrates the reproducibility of right atrial STE for elucidation of right atrial strain. In this study, the endocardial boundaries or edges of the right atrium were manually contoured which gave the speckle tracking algorithm the closest estimate of the boundaries of the right atrial endocardium. From these initial guides, the algorithm "tracked" the consistent speckles frame by frame throughout the cardiac cycle. The output was, after mathematical calculations (cross-correlation techniques and the sum of absolute difference), in the form of strain and SR curves and global and segmental values. The segmental values showed high variability and little agreement and are not reported here.

The results of the reproducibility study show poor agreement of inter-observer and intra-observer values for global longitudinal strain and SR values. The technique has wide limits of agreement which mean that it is not very reproducible. This is specially the case when image quality is poor or images are acquired focused on left ventricle. The fact that the right atrium has very thin walls makes it difficult to track as compared to other chambers. If there were image quality issues, these would affect the right atrial

strain more than other chambers. Placing tracking points at different atrial locations makes greater difference in the right atrium than in any other chamber.

In brief, the right atrial strain through 2D STE right atrial strain is a poor method of measurement of mechanical function of the right atrium. But the main limitation of our study was absence of focused views of the right atrium and relatively small numbers. Therefore, further studies are needed to prove or disprove this interesting area of cardiac physiology and mechanics.

Chapter 4

The Reference Ranges for Right Atrial Strain

4.1 Introduction

Although normal reference ranges for the left ventricle,[100] the right ventricle and the left atrium have been defined, more work still needs to be done to determine normal ranges for right atrial strain to aid the use of right atrial strain as a well-validated clinical tool. We, therefore, require well-validated normal reference ranges in normal hearts to allow comparison of normal ranges with various disease pathologies like atrial fibrillation,[97, 101, 102] pulmonary hypertension[78], and fibrotic right-sided heart diseases like inflammatory myopathies.[63] The aim of this study was to generate a normal range for the standard right atrial strain measures and determine the effect of age, gender and BMI on strain parameters.

4.2 Methods

4.2.1 Patient Characteristics

28 subjects were included in the analysis as a part of ongoing approved trials. Study individuals were defined as having no cardiac disease as evidenced by normal ECG and normal trans-thoracic echocardiogram, absence of liver and kidney disease on routine testing. No relevant family history was present. Basic demographics of the cohort are given in Table 4.1 below.

4.2.2 Statistical Methods

For statistical analysis, SPSS software version 20 was used. Continuous data were described as mean +/- standard deviation while categorical data were presented as a median and inter-quartile range. A Kolmogrov–Simonov test and Shapiro–Wilk test were used to check for normality of data while Q-Q plots were used to confirm normal distribution.

4.3 Results

4.3.1 Normal Reference Ranges

The data were largely normally distributed as shown in the normality plot (Q-Q) plot in figures 4.1 and 4.2. The demographic features of the individuals are given in Table 4.1, which shows that the group consists of young to middle aged healthy non-obese individuals. The studied echocardiographich parameters are described in Table 4.2, which shows normal left ventricular structure and function for the given age and gender.

The speckle tracking-derived strain parameters for the right atrium are given in Table 4.3 and are compared with left atrial strain in Table 4.4.

Table 4.1.Characteristics of the population

Parameter(n=28)	Mean	SD
Gender	5 males, 23 females	*
BMI	25.7	5.7
Age	41.9	8.2

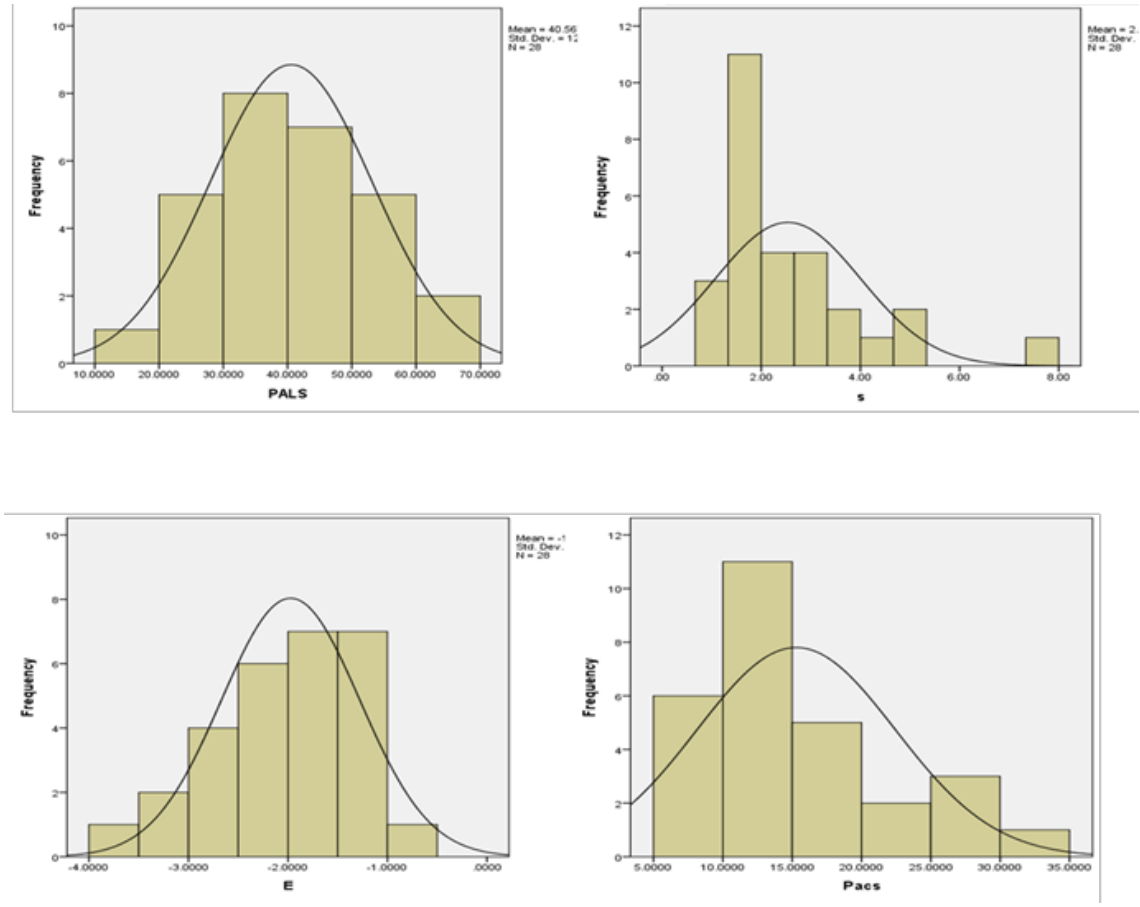


Figure 4.1. Histogram with Normality Curve of PALS, PACS, S`, E, A`.

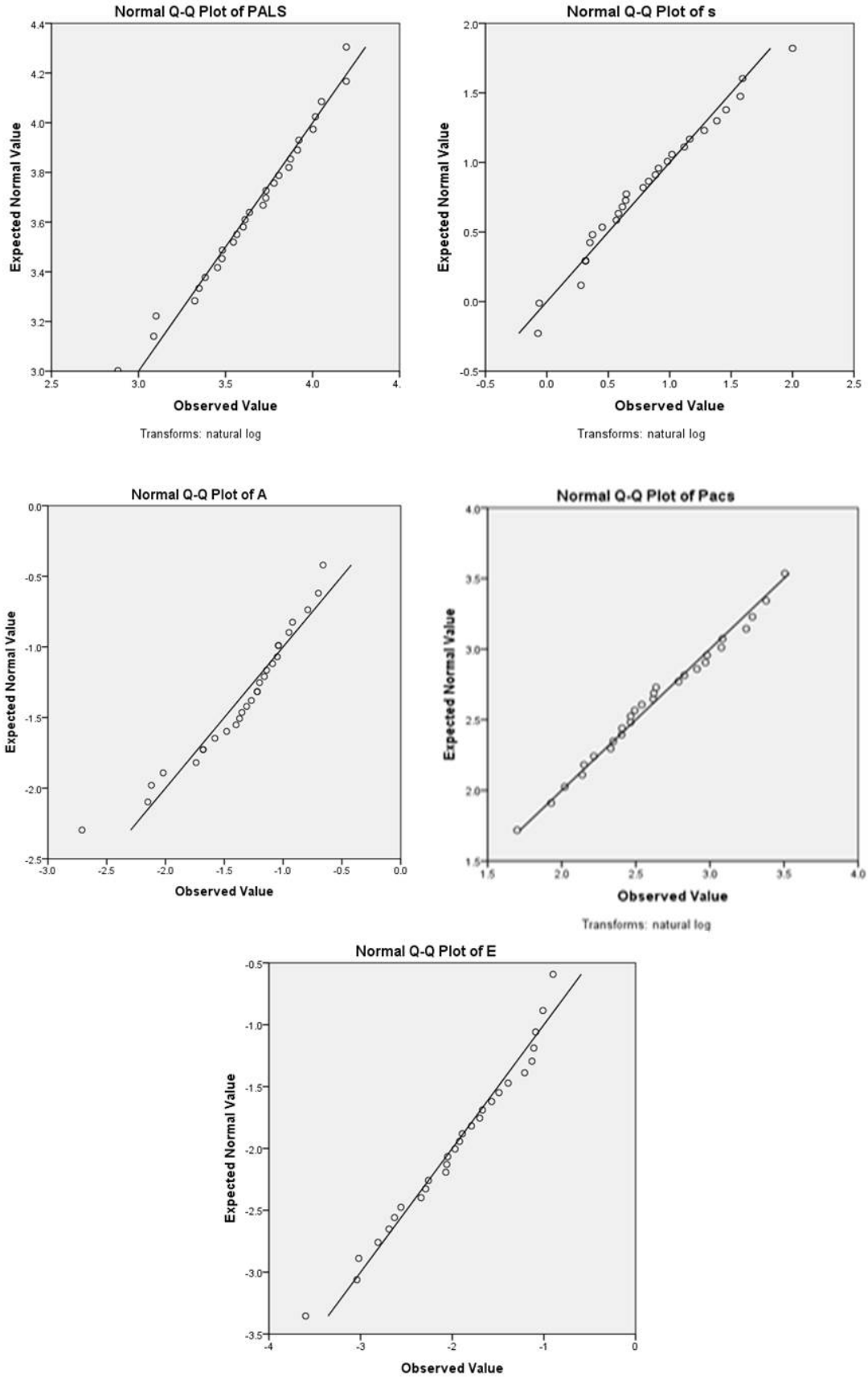


Figure 4.2. Q-Q plots of PALS, PACS, S, E, A

Table 4.2. Echocardiographic Parameters. IVSd (Interventricular septum diameter in diastole in cm), LVIDd (Left ventricular internal diameter in diastole), LVPWd (Left ventricular posterior wall diameter in diastole), MVE (Transmitral early diastolic velocity), MVA (Mitral valve late diastolic velocity), DECT (Deceleration time), E/A (E to A ratio), Sm Tissue Doppler systolic velocity, Em (TDI Early diastolic velocity), Am (TDI late diastolic velocity)

Parameter	Mean	Standard Deviation
IVSd (cm)	.85	.197
LVIDd (cm)	4.39	.459
LVPWd (cm)	.88	.193
EF (%)	47	27
MVE (Cm/s)	71.08	16.137
MVA (Cm/s)	53.92	15.195
DECT(cm/s2)	.18	.044
E/A	1.37	.314
LateralSm (cm/s)	10.03	2.803
LAteralEm(cm/s)	12.98	3.537
LateralAm(cm/s)	8.38	2.020
SeptumSm (cm/s)	8.30	1.217
SeptumEm (cm/s)	10.49	2.129
SeptumAm(cm/s)	7.52	2.080

Table 4.3. Longitudinal Strain Parameters for the right atrium PALS = Peak Atrial Longitudinal Strain, PACS = Peak Atrial Conduit Strain, S` = the reservoir phase SR, E` = the conduit phase SR, A` = booster pump SR

Parameter	Mean	Std. Deviation
PALS (%)	46.76	18.71
PACS (%)	27.61	10.10
Atrial kick	-6.67	-4.01
S (1/s)	1.88	0.46
E (1/s)	-1.64	-0.58
A (1/s)	-1.24	-0.26

4.4 Discussion

Padelleti et al[84] have recently reported the values for right atrial strain through STE using Echopac software. The values reported are somewhat higher than in our study. One of the possible explanations could be the different vendor and analysis software used (Echopac). Quintana et al described the right atrial strain through Doppler echocardiography and reported a relative contribution of the roof, lateral walls, inter-atrial septum and tricuspid annulus.[1] D'Andrea described right atrial strain in a mixed population of normal individuals and those with dilated cardiomyopathy (DCM) before and after CRT.[85] Moreover, there is more variability between different individuals as compared to other chambers due to thin atrial walls, characteristic anatomic features, electrophysiological phenomena which originate in the right atrium, image quality issues and usual confounders such as atrial volume, gender, age and BMI.

Speckles are noise in the image and many steps including image acquisition, image storage, image processing, and image transfer alter the quality of the image and hence strain recordings. Atria being small are more prone to errors in measurement than ventricles by this image processing. This is because speckle tracking algorithms track blocks and kernels of pixels and find the correlation or the sum of least squares to find a match. The larger the block the higher the chances of finding an adequate match.

Although left ventricular strain as previously reported is higher in females compared to males there were statistically significant differences in left ventricular longitudinal strain, which fits well with the picture that premenopausal women have a better cardio metabolic profile than males. In the study by Padelleti et al, however, this pattern does not seem to exist in the right atrium where there is no statistically significant difference in the parameters between males and females. Right atrial strain as an index of

pulmonary artery systolic pressure in diastolic heart failure (DHF) has also been validated.[103]

Table 4.4. Comparison of right atrial strain values from previous study[84] and our study.

Parameter	Padelleti et al[84]	Our Study
PALS (%)	49±13	48+/-18
PACS (%)	8±6.38	27+/- 10
S (1/s)	2.12±0.58	1.88+/- 0.46
E (1/s)	−1.91±0.63	-1.64+/-0.58
A (1/s)	−2.18±0.78	-1.24+/-0.26

We have defined normal reference ranges for right atrial strain parameters on a carefully selected cohort of healthy individuals with high quality images. Our results are in close agreement with the previously reported study by Padelleti et al.[84] However, there is a massive difference in conduit strain, which can be explained, by the difference in technique for measuring the conduit phase strain. Padelleti et al have taken the Peak Atrial Longitudinal strain as the point of peak reservoir phase and we have followed the same convention.

However, they have measure Peak Atrial "contractile" strain(PACS) to represent the conduit phase strain. The term "contractile" is misleading here as the phase which is shown in the paper by Padelleti et al (shown below) refers to conduit phase and not the booster pump (the actual contractile phase). Moreover, they have measured the PACS (Peak Atrial Conduit Strain, as we have called it, to clear the confusion) in an arbitrary manner. We have measured the time of peak early strain rate E` corresponding to conduit phase and then measured the strain at the same time point on strain curves. That is why our values are different from their groups values in terms of conduit strain.

One of the major limitation of the study was small sample size due to strict criterion to get highly filtered high quality image results and predominantly female population which would not represent entirely a "normal" cohort.

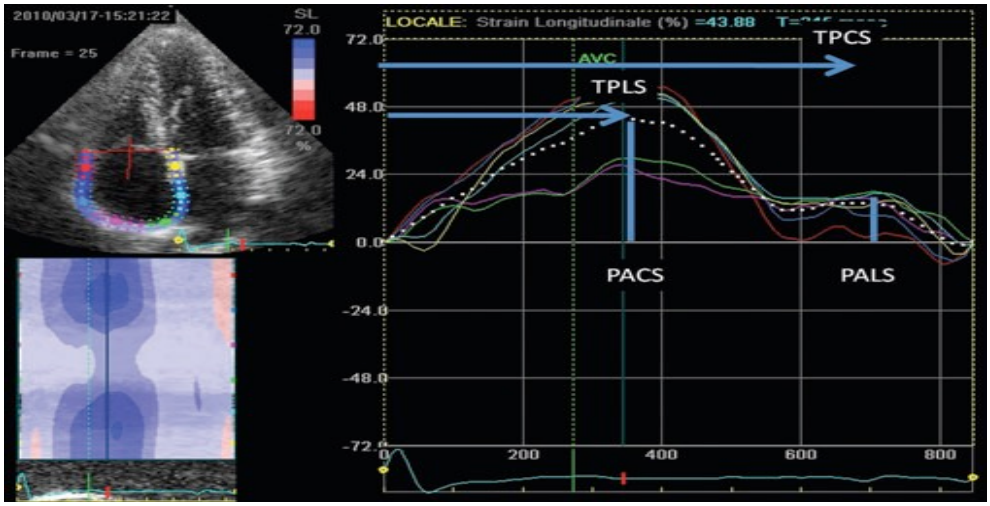


Figure 4.3. PACS And PALS as defined by Padelleti et al. [84] Please note there is no Booster pump mentioned in the figure

Chapter 5

Comparison of Echocardiography and CMR-derived Atrial Deformation Parameters

5.1 Introduction

Comparative volumetric studies of LV have been done through CT scan,[104, 105] cardiac catheterisation scintigraphy, 2D[106], 3D[106, 107 108], M-mode echocardiography, stress echocardiography[109] and MRI.[16, 108, 110-114]

Volumetric studies provide useful information about the structural aspects of the heart but comparative studies of the right atrium are largely lacking. To some extent, this is because imaging modalities other than echocardiography struggle to explore right atrial myocardial mechanics.

Feature tracking or feature extraction is a sub-form of optical flow techniques and broadly speaking optical flow technique detects the flow or movement of each pixel in space and time about brightness and darkness of the image. Feature tracking software or algorithms detect important features such as edges and corners and tracks them on a frame-by-frame basis. It has been successfully applied to evaluate the mechanics of MR cine images.

Feature tracking-derived CMR is a new emerging modality, which combines the strengths of CMR with image processing capabilities without the issues of image quality[115-118].

We therefore compared the values of right atrial strain derived by STE to those derived from feature tracking CMR.

5.2 Methods

5.2.1 Sample Size

We had 31 healthy volunteers, all females aged 30 to 63 years who had participated in the study and who had undergone echocardiography and CMR on the same day.

All subjects gave informed consent and the local research ethics committee approved the research protocol.

Patients who were taking any cardiovascular medications were not included in the analysis of this study. Similarly, subjects with any structural heart disease such as valvular heart disease, cardiomyopathy, pericardial disease and ischemic heart disease were not included in the analysis. Moreover, only those subjects were included in the analysis that were free from liver, kidney and lung disease, as assessed by history and physical and routine investigations.

5.2.2 Echocardiography Protocol

Echocardiography was performed on Toshiba Artida (Toshiba Medical Systems, Netherlands) as described in Chapter 2.

5.2.3 MRI Protocol

All CMR exams were performed at 1.5-T (Sonata, Siemens Medical Solutions, Erlangen, Germany). Steady-state free precession cine images (echo time/repetition time 1.5/3.0 ms, flip angle 60°) were acquired using the long horizontal axis (HLA) view. The right atrium was visualised in HLA view.

5.2.3.1 *Image Analysis*

Tomtec (Diogenes Medical, Germany) is vendor-independent software which can accept and analyse cines from any MRI platform. The digitally stored data was uploaded to the Tomtec server. The user then selected the appropriate study and the image and program was initiated. On the user interface options, there are options for selecting a suitable view, adjusting the grey level and making the Endocardial borders visible. The user can also select to manually contour the endocardium or draw it in a semi-automated fashion. Any phase of the cardiac cycle can be selected. For the purpose of our study we selected the point where atria were fully expanded and the Endocardial border was fully visible.

The endocardium and epicardium were traced by placing small dots (kernels) on the lining. Then the algorithm was run, which gave the visual map of strain, SR, velocity, and displacement. Volume curves were also calculated but were not used in our analysis.

Regional and global strain with time-to-peak information was calculated in the next step.

The segment representing fossa ovalis was excluded from the analysis due to poor tracking and thin walls

5.2.3.2 *Feature Tracking Algorithm*

Unlike HARP[119, 120], SENC, DENSE[121], SPAMM, C-SPAMM and other tagging analysis methods[122, 123] which "detect" the border through perturbation or destruction of magnetization and measure strain through two step imaging and complex post processing , in feature tracking the borders are "tracked" during post processing in three steps which are computationally simple and efficient time wise. First, there is one-dimensional tracking through the line of the trans mural cut. A line is drawn orthogonal

to the trans mural plane and the image is divided into columns by a line five pixels thick. This is a form of M-mode representation and then feature tracking is performed.

The next step involves optical flow technique where the adjacent frames are tracked based on best fit criterion and the presence or absence of features in a 2*2 dimension.

The third step is used to detect twist and torsion and is a combination of steps 1 and 2 with minor modifications.

5.3 Results

The demographics of the females undergoing CMR and echo examination are shown in Table 5.1. They are normotensive, middle aged and slightly overweight. The values for feature tracking-derived MR strain are shown in Table 5.2. The values are 10–15% lower compared to speckle tracking-derived echo strain.

Table 5.1. Demographics of Females undergoing CMR Examination.

Parameter	Mean	SD
N	31	*
Age(years)	42	4
Height(feet)	1.6	0.05
Weight(Kg)	70.3	15.6
BMI(Kg/m2)	25.8	5.6
SBP(mm of Hg)	121.3	13.2
DBP(mm of Hg)	74.2	9.7

Table 5.2. Limits of Agreement and Bias of Between Strain and SR Parameters derived by Echocardiography and CMR.

Parameter	Limits of agreement	Bias
PALS (%)	22.8, -57.6	-17.8
PACS (%)	15, -23	-4.3
S`(1/s)	4.9, - 0.9	2
E`(1/s)	-0.2 , -3.3	-1.8

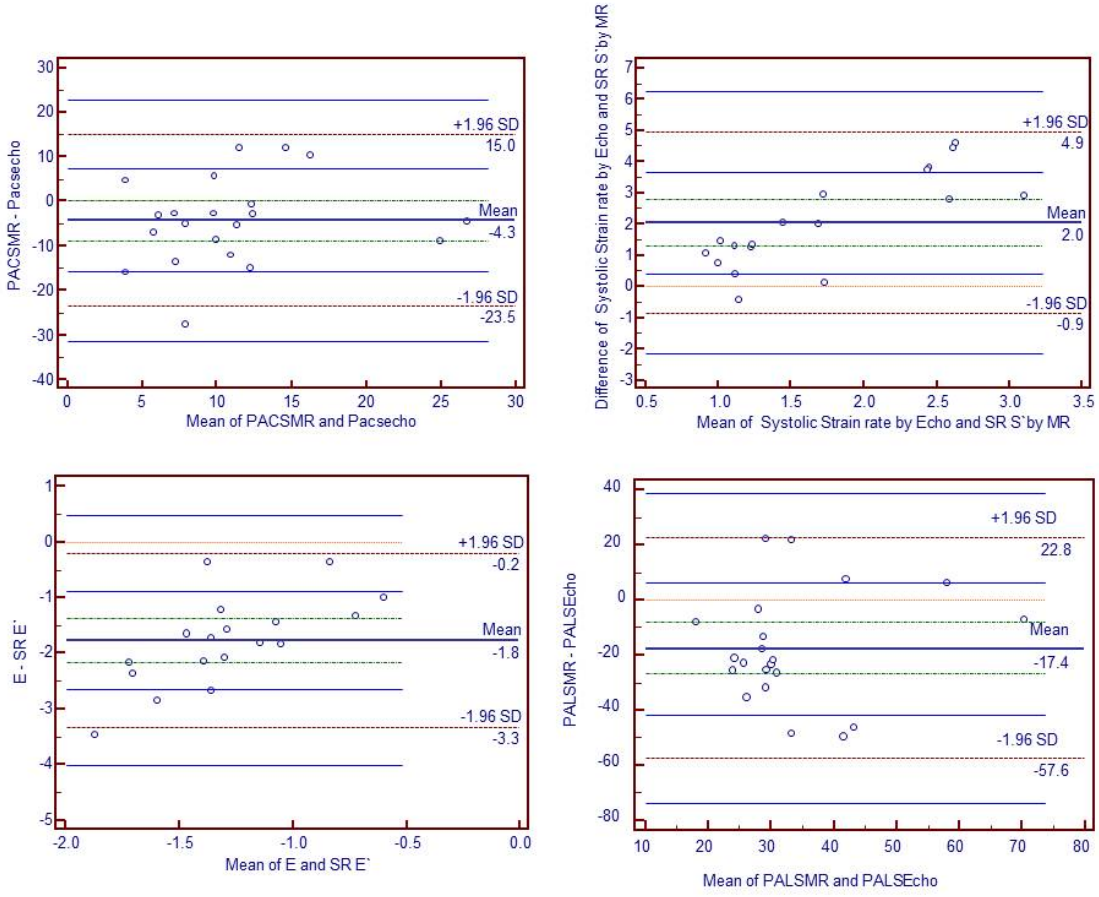


Figure 5.1. Bland–Altman plots of PALS and PACS, S` and E` between Echo and CMR showing acceptable BIAS and relatively wide limits of agreement showing poor Interobserver agreement.

5.4 Discussion

Feature tracking is an established image analysis technique, which is a subcategory of optical flow analysis.[116] It involves detection of edges, borders, and corners of an object and, in the case of the heart, it involves consistent features of the heart such as papillary

muscles and trabeculations of the heart. LV strain has been validated through FT in healthy individuals, for Duchene Muscular Dystrophy[117] during dobutamine stress testing,[118] viability assessment in ischemic dilated cardiomyopathy and scar quantification.[124] CMR Volumes and 3D Speckle is tracking echo-derived volumes and have been compared and shown to have good agreement and inter-test variability.[35] Feature tracking CMR has also been compared with MR tagging and has been shown to have good agreement for circumferential and longitudinal strain as compared to radial strain.[115] However, studies comparing speckle tracking echo and feature tracking CMR are scarce. To the best of our knowledge, this is the first study to compare right atrial strain measurement through ST Echocardiography and Feature tracking CMR.

There are two main findings of our study: 1) the strain derived from feature tracking CMR is lower than the strain derived from speckle tracking echocardiography; and 2) there is poor agreement between STE-derived strain and FT-derived strain for various phases for the atria.

The reasons for these findings can be twofold. STE uses high frame rates in the range of 60 to 90 FPS while MRI has low temporal resolution and uses low frame rates of up to 30FPS. The speckle tracking algorithm calculates strain by block matching of consistent speckles in each frame of the entire cardiac cycle. More frames means more blocks, which would lead to a higher string value. Our groups' unpublished data have shown that in the same individual higher frame rate lead to a higher strain under similar conditions. Moreover, the speckle size, speckle distribution, speckle arrangement, coherence and decoherence pattern of the scattered echo waves are also responsible for differences in echo and CMR strain. While considering CMR, artefacts of various types, shimming, noise levels, RF interference pattern, image sequence type, the T1 and T2

relaxation times of various tissues, and heating of the coils may also affect the final image formation and the pattern of features that is being formed.

Thin atrial walls leading to suboptimal tracking are also an important reason for poor agreement between echo and CMR parameters. Another reason for wide variation in results and poor agreement was that echo and CMR scans could not be acquired in the same plane due to patient position in scanner vs. echo machine, breath hold techniques, acquisition at different time points to name a few. Different planes presented different anatomical structures fitted in small space and made agreement even more difficult and poor.

STE-derived strain is systematically higher than FT-derived CMR strain.

Chapter 6

Right Atrial Strain in Heart Failure with Normal Ejection Fraction

6.1 Introduction

Heart failure has high mortality and morbidity.[125] According to some sources, the prevalence of Heart Failure with Normal Ejection Fraction (HFnEF) may reach up to 50% of heart failure patients.[126] Patients with HFnEF have almost same prognosis as those with heart failure with reduced ejection fraction (HFREF).[126, 127] Various hypotheses shedding light on mechanistic insight into the HFnEF have been successfully tested. These include alterations in the left atrium[128] and left ventricular size,[129] wall motion abnormalities,[130] energetic changes,[131, 132] electrical phenomena[133] and flow abnormalities.[134]

The typical patient is an old-aged female with late onset hypertension, obesity, anaemia, renal failure with diabetes and who has a right bundle branch block or atrial fibrillation with no history of ischemic heart disease. These patients have left ventricular hypertrophy with dilated left atria and impaired relaxation and increased stiffness of the left ventricular chamber. The increased filling pressures are a cornerstone of the pathophysiology but are considered an effect rather than the cause of relaxation abnormalities. Although several studies have been done on left ventricular hemodynamic in HFnEF,[48, 83, 85, 127, 128, 135-147] very few studies have explored right-sided heart function in HFnEF.

Conventional echocardiography[148] has been the cornerstone for the evaluation of HFnEF, but STE has shown some promise in difficult-to-diagnose cases and patients with subtle disease and normal echocardiographic parameters. STE, with parameters like strain, SR,[149] twist, untwist rate and torsion,[150, 151] which measure cardiac deformation in all directions independent of angle of insonation, has been shown to be an emerging modality to study cardiac mechanics.

We hypothesised that HFnEF abnormalities are not restricted to the LV and LA but involve the most upstream chamber the RA as well.

Right atrium has a vital role in HFnEF because it is the source of atrial fibrillation, which worsens heart failure, and BNP and NT-pro BNP, which correlate quite strongly with left ventricular filling pressures and are routinely used as a biomarker of HFnEF. These are produced from left and right atria from neurosecretory granules, which were briefly mentioned in the histology section in Chapter 1.

6.2 Methods

6.2.1 Sample Size

27 healthy controls and eight HFnEF patients recruited in a clinical study were analysed.

The criteria used to diagnose HFnEF are shown in Figure 6.1.

6.2.2 Study Procedure

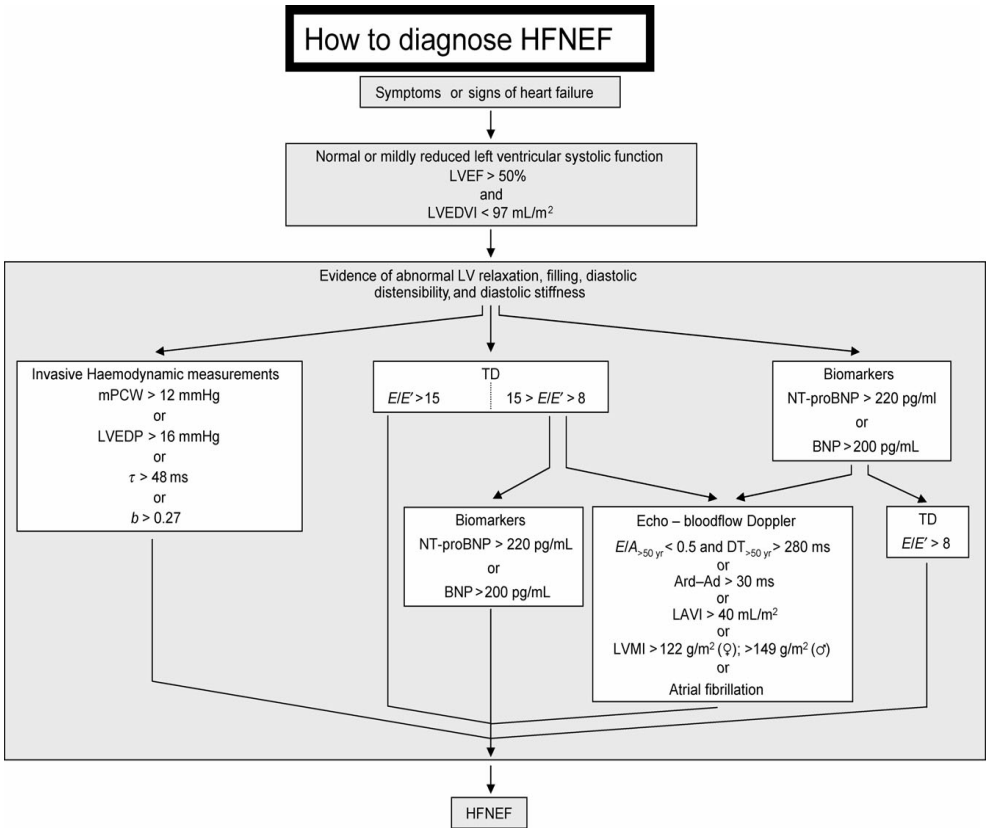


Figure 6.1. Reproduced from Paulus et al: How to diagnose diastolic heart failure : A consensus statement on the diagnosis of heart failure with normal left ventricular ejection fraction of the heart failure and echocardiography associations of the European society of cardiology. European Heart Journal. 2007; 28: 2539–2550

Table 6.1. Demographics of the normal cohort

	Mean	**Std. Deviation**
Age (years)	50	15.6
Gender	14 males/10 females	-
HR (beats/min)	74.91	15.476
BSA (m^2)	2.00	0.0
LAVI	19.45	9.723

Out of seven patients, 2 were hypertensives, one was diabetic, three had high cholesterol levels, all of them were in NYHA class 2. Three of them were taking Beta Blockers, 4

were on statins,2 were taking ACE inhibitors,one was taking Calcium channel blockers,6 of them were taking proton pump inhibitors,

6.2.2.1 *Echocardiography*

Apical four-chamber data were collected as described in Chapter 2 on a Philips ie33 machine.

6.2.2.2 *Image Analysis*

Images were analyzed using Tomtec cardiac performance analysis software (Tomtec, Germany).

6.3 Results

The data were normally distributed as shown in the figures below, passing the Shapiro–Wilks test of normality.

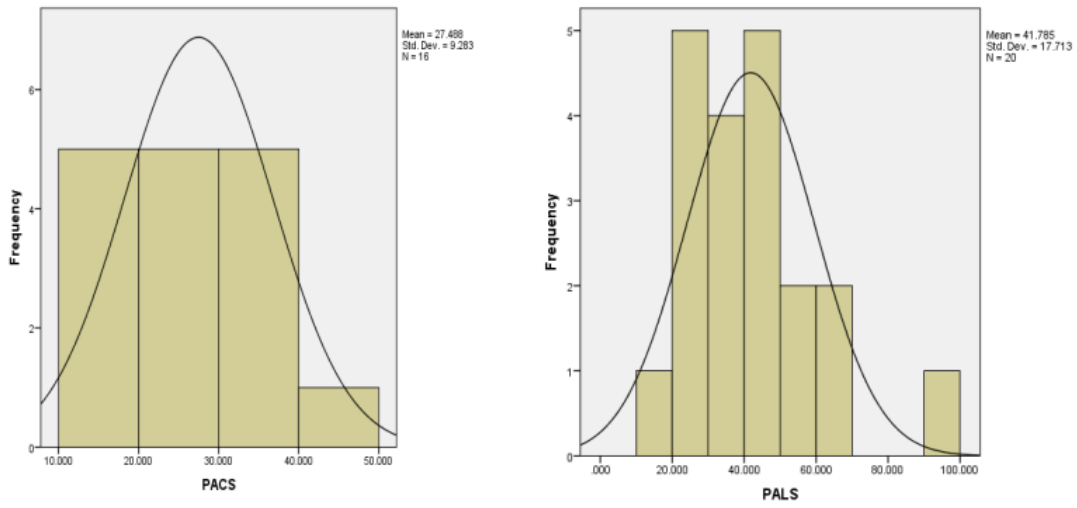


Figure 6.2. Histogram with normality curve showing normal distribution of strain data

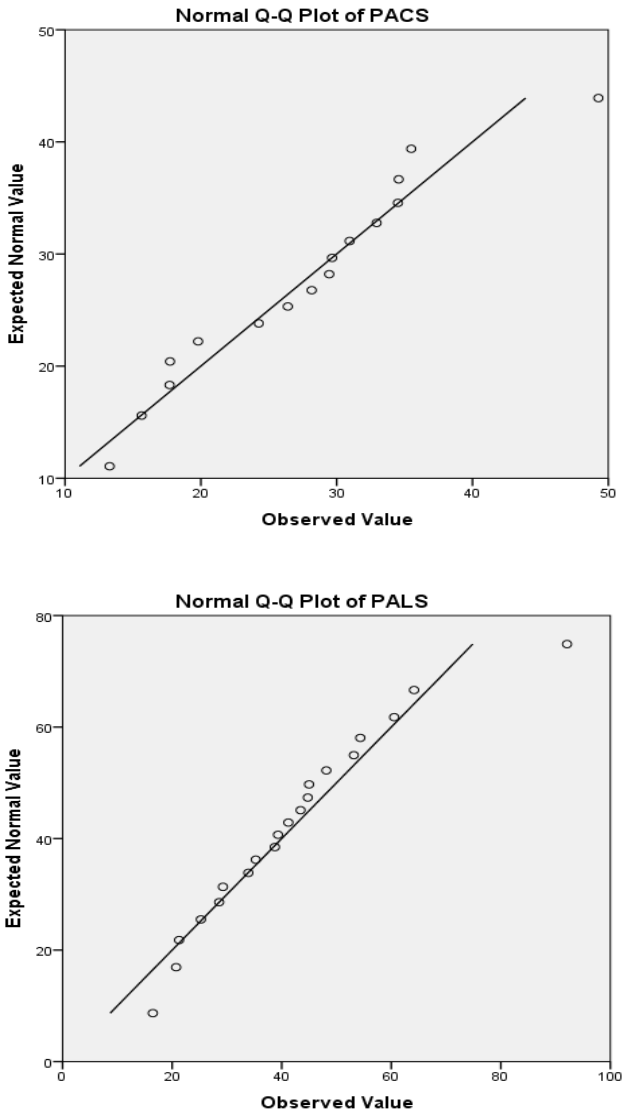


Figure 6.3. Q-Q Figure 6.4 Q-Q plots of PALS showing its normal distribution plot of PACS showing its normal distribution

The reservoir phase and the conduit phase of the right atrial function decreased to a statistically significant level in patients with HFnEF as compared to the normal controls.

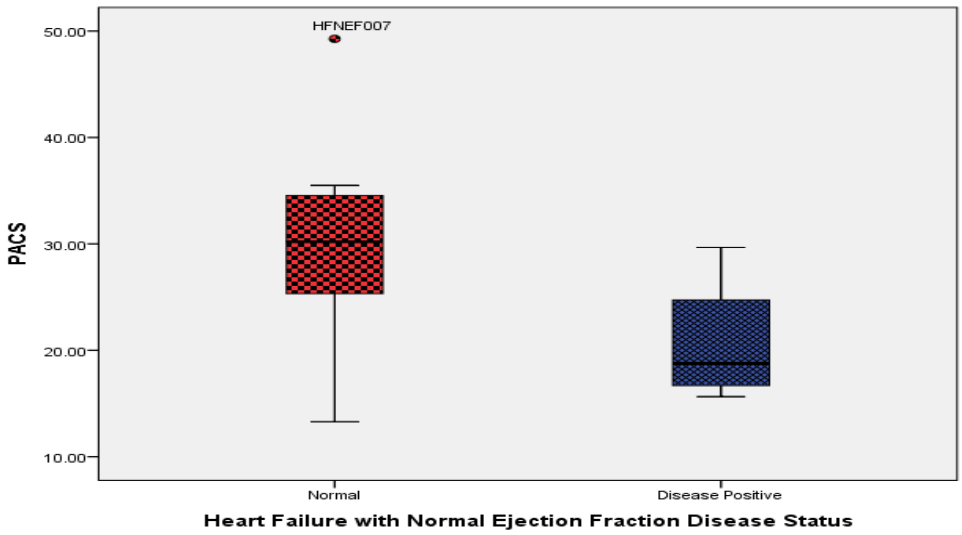


Figure 6.4. Box plot showing the decreased conduit function of the right atrium in HFnEF patients as compared to normal controls.

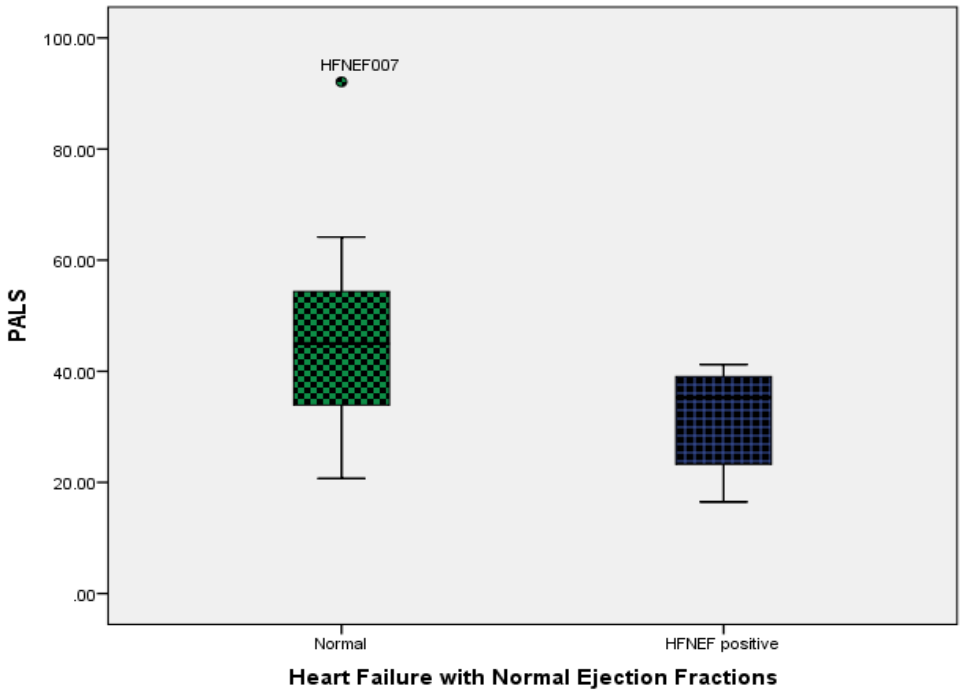


Figure 6.5. Box plot showing decreased reservoir function of the right atrium in HFnEF patients as compared to normal controls. The box plot shows that the meadian of the two groups(healthy controls and HFNEF) don't overlap, this is because the dispersion of the HFNEF group is very small specially in the upper quartile . The upper whisker of the HFNEF group is very small and the medians or whiskers don't overlap hence we get aa p-value of 0.05

Table 6.2. Comparison of various strain parameters between healthy controls and the HFnEF group

Parameter	Healthy Mean (SD)	HFnEF Mean (SD)	P-value
PALS	47.54(18.56)	31.07(9.91)	0.01*
PACS	29.74(9.20)	20.70(6.20)	0.05*
Atrial Kick	-5.70(4.21)	-11.30(10.20)	NS§
S`	1.86(0.40)	1.97(0.83)	NS
E`	-1.73(0.56)	-1.45(0.72)	NS
A`	-1.50().49)	-1.51(1.73)	NS

6.4 Discussion

One of the main findings of our study is that right atrial longitudinal strain is decreased between HFnEF and healthy controls. More specifically, the reservoir and the conduit function are decreased, while the atrial kick is similar between the two cohorts. Similarly, SR is also not different statistically between the two groups.

Although left heart function has been studied extensively through echocardiography,[146, 147, 152-155] there has been little attention given to the atria in DHF,[143, 156] especially the right atrium. If we look at the mechanistic aspects of the right atrium in heart failure, it is closely interrelated with atrial fibrillation and diastolic dysfunction.[157] Because of heart failure, the atria first hypertrophy and eventually dilate[158, 159] due to pressure overload and to some extent volume overload of the right-hand side of the heart. This results in deviation from the normal electrical conduction where electrical wavelets follow a specific path of fixed length but different morphology. With chamber dilation, the path length is increased and so the chances of re-entry and abnormal phenomenon are increased.[160]

It has been shown in many studies that longitudinal function of the left atrium and left ventricle is decreased in HFpEF,[83, 128, 130, 139, 161-164] so our finding of decreased longitudinal function of the right atrium is in harmony with the previous findings. The

longitudinal function in the left ventricle is mainly governed by the innermost endocardial fibres and these are the fibres affected in sub-endocardial infarcts. Nevertheless, arrangement of fibers in the right atrium is not as straightforward as it is in the left ventricle and different anatomical structures and embryological remnants contribute to atrial morphology and hence strain.

A few studies have been done on left atrial reservoir function showing decreased reservoir function in heart failure. [165, 166] However, to the best of our knowledge this is among the very first studies exploring right atrial mechanics of HFnEF patients with healthy controls through STE. Our results show that HFnEF is a generalized process, which not only affects the left ventricle and the left atrium but also the right atrium as well. One explanation for the involvement of the right atrium might be that we have chosen a highly specific cohort of HFnEF patients who have pure HFnEF, hence the patients showing involvement of the right heart/the right atrium because of left heart failure.

Previous studies have shown that in the LV one of the earliest changes is impaired relaxation, which occurs due to impaired calcium handling and contractile fibre cycling or deficient structural protein iso-forms such as titin. We hypothesize that a similar mechanism occurs in the right atrium as well, where the reservoir function – on which other two phases of atrial physiology are dependant – is the first one to be affected.

In conclusion, the reservoir and the conduit function of right atrium is decreased in patients with HFnEF. STE is a robust technique, which is well suited to detecting the decreased function before the volumes are actually changed and atrial fibrillation may result from these mechanical changes.

Chapter 7

Right Atrial Strain in Rheumatoid Arthritis

7.1 Introduction

The inflammatory arthropathies and systemic rheumatic diseases are associated with Increased rates of cardiovascular disease even in the absence of traditional risk factors.

7.1.1 Rheumatoid Arthritis

RhA forms the major disease burden of these inflammatory cardiomyopathies. RhA generally leads to two types of cardiomyopathies. A non-specific inflammatory cardiomyopathy (dilated cardiomyopathy) or a specific granulomatous cardiomyopathies, which is marked by granulomata formation in the myocardium[167]. RhA has significant pulmonary involvement (pulmonary hypertension) leading to hypertrophy and eventual dilatation. The back pressure generated also involves the right atrium, hence, the right atrium acts as a barometer and volume sensor of the pulmonary circulation. Padelleti *et al* have shown that right atrial strain in a normal population is a good surrogate measure of pulmonary artery systolic pressure as measured by right heart catheterization[103].

Left ventricular diastolic dysfunction (DD) (as evidenced by altered transmitral velocities, E/A ratio, E/E`, pulmonary wave waveform and velocities, deceleration times, and Tissue Doppler indices namely S`, E` and A` waves) is more prevalent in rheumatoid patients than healthy controls. The degree of DD correlates with IL-6 levels

and disease duration. The association remains significant after controlling for cardiovascular risk factors.[168] The radial and longitudinal global and segmental strain has been shown to be decreased in RhA patients even in the absence of cardiovascular disease or risk factors and otherwise normal echocardiography parameters.[63] It has been shown that LV end systolic longitudinal and radial strain has been decreased in RhA patients despite normal echocardiographic parameters[63]. Another recent study showed decreased RV and LV global longitudinal function in RhA patients as compared to healthy controls and the deformation parameters correlated well with the disease severity[64].

According to another study, RhA patients have decreased sub clinical strain parameters which are associated with Nitro-oxidative stress and decreased endothelial function, this function improves by administration of Anakinra, a drug which selectively blocks IL-1 function[65].

Pulmonary hypertension is a rare finding in RhA and is characterized as a mean PA pressure ≥25 mm Hg at right heart catheterization.[169] There is not only LA dilation but also electromechanical delay and disruption of LA function in RhA.[170] The neglected RV chamber has not been studied in as much detail as the LV and the LA in RhA. A study by Birdane et al has shown that there is bi-ventricular involvement in RhA. Since previous studies have shown that LA is also involved, the next most logical step is to look at the most neglected chamber of the heart, i.e. the right atrium. Conventional echocardiography can only measure the area and volume of the right atrium but STE is very well suited to exploring the mechanistic aspects of the right atrium. Therefore, in this study we explored the mechanical function of the right atrium through STE.

7.2 Methods

There were 33 participants selected for analysis: 9 Rheumatoid Arthritis and 24 healthy controls.

7.2.1 Setting

All studies were performed in a tertiary care hospital (the John Radcliffe Hospital, Oxford), at the Cardiovascular Clinical Research Facility (a dedicated research facility).

7.2.2 Study Procedure

7.2.2.1 *Echocardiography*

We acquired an apical four-chamber view in 2D using the Toshiba Artida system.

7.2.2.2 *Image Analysis:*

Images were analyzed using Tomtec cardiac performance analysis software (Tomtec, Germany).

7.3 Results

The curves for normality are given in the figure below.

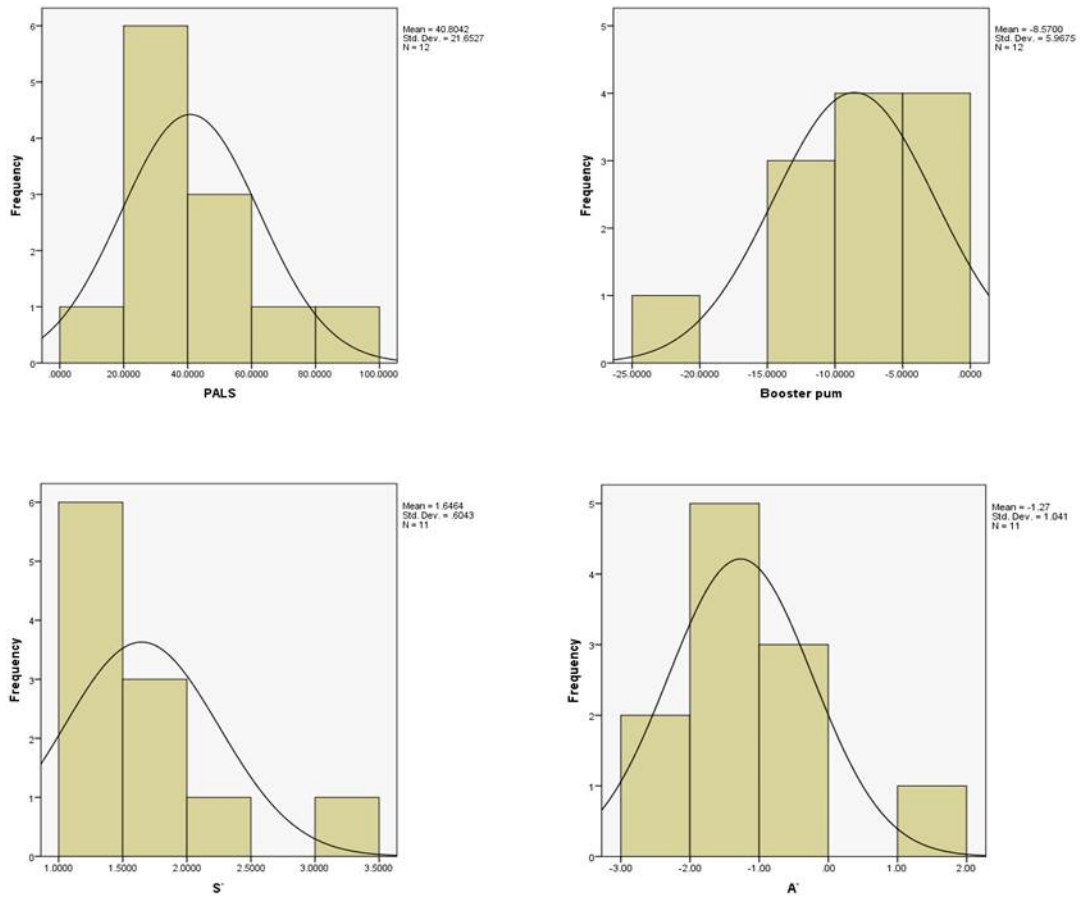


Figure 7.1. The Bar chart with normality curves for the S`, A`, Booster pump and PALS: The curves show that data is normally distributed with major peaks in the centre of the the Gaussian distribution curve.

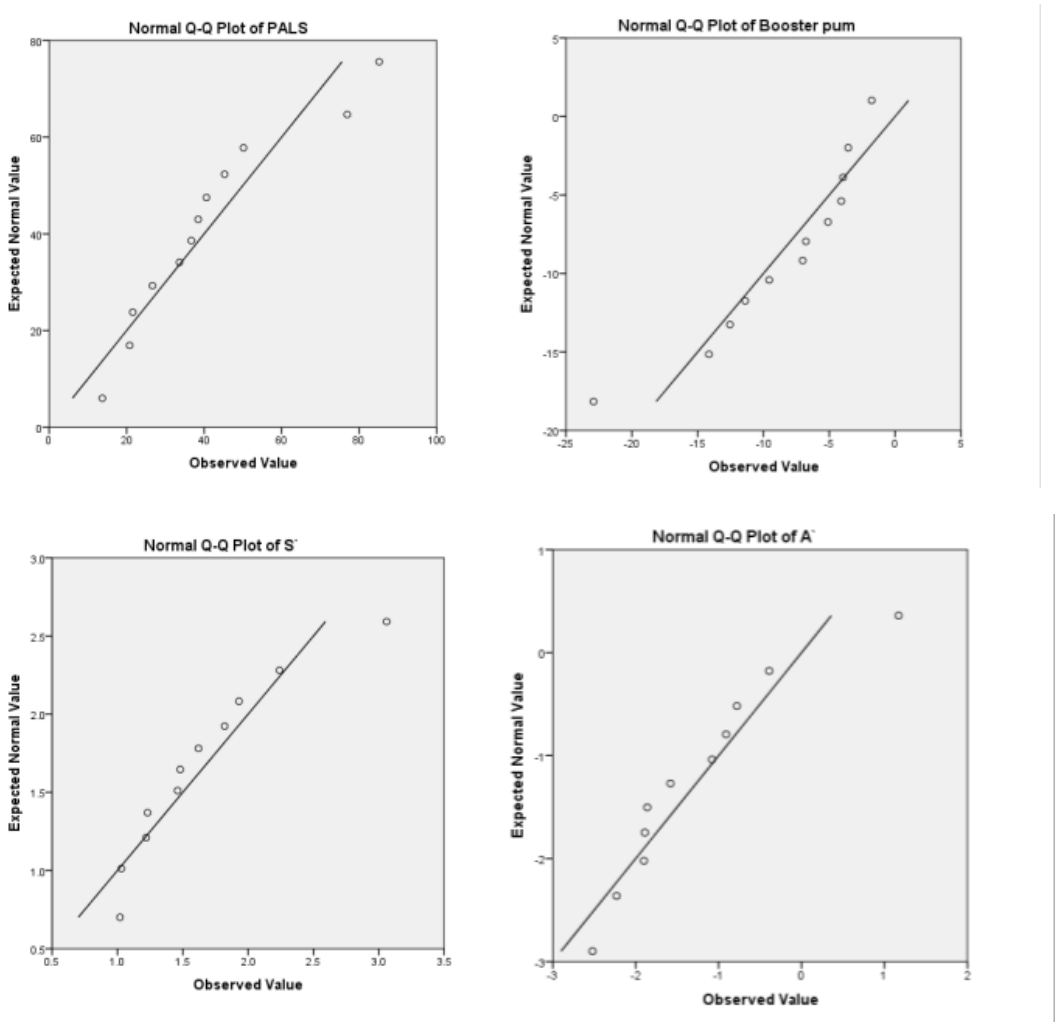


Figure 7.2. Q-Q plot of the strain and SR parameters : The Q-Q Plot which plot the observed value against the expected value are shown in the above figure. The less deviation of the points from the trend line points towards normality of the data.

The average duration of illness was 8 years, mean age was 42 years, all the patients were on methotrexate, 2 were taking sulfasalazine, 6 were taking chloroquine, 1 out of 8 patient was on prednisone, Average duration on Disease Modifying Antirheumatic drugs was 5 years, 4 had coronary artery disease but were mainly free from symptoms of the coronary disease, half of the patients had positive family history for ischemic heart diseases. Two had liver disease.

Table 7.1. Mean and standard deviation of strain parameters of healthy controls and Rheumatoid Arthritis patients . There is no statistically significant difference between any of the parameters for the right atrium.The Conduit phase strain (E`) could not be measured from the strain rate wave forms. Since the timing of conduit strain is derived from E` (conduit strain rate) peak timing. The conduit strain could not be measured either.

Parameters	Healthy Mean(SD)	RhA Mean(SD)	P-value
PALS	50.18(20.44)	36.11(23.11)	NS
Booster Pump	-9.93(6.34)	-5.84(4.67)	NS
S`	1.62(0.41)	1.69(0.92)	NS
A`	-1.35(1.21)	-1.12(0.79)	NS

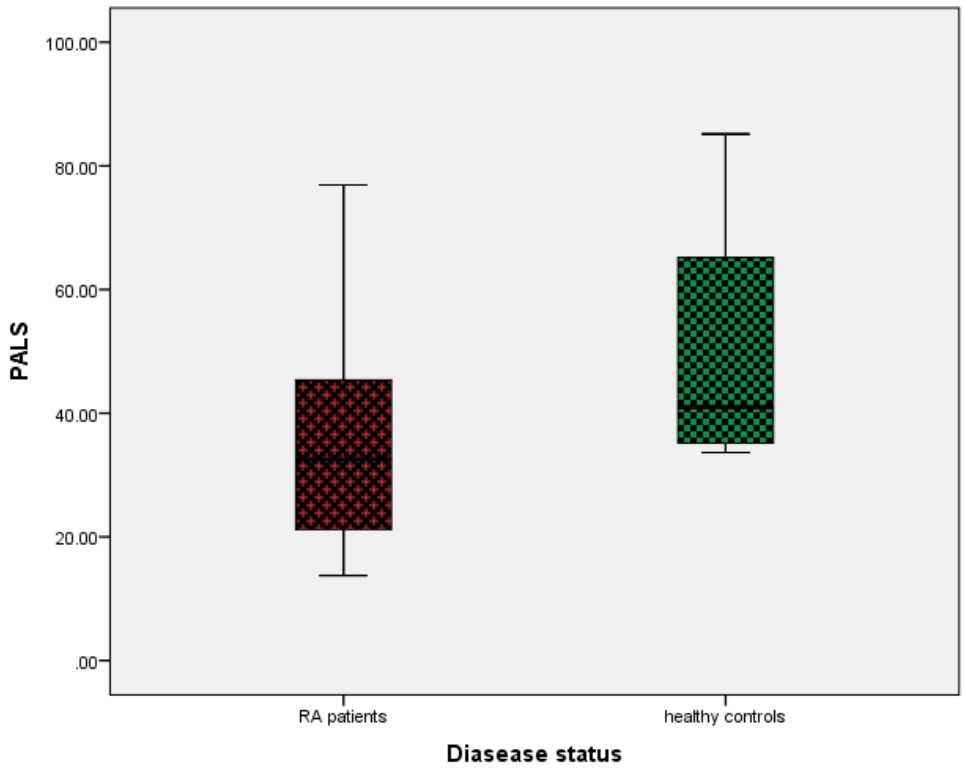


Figure 7.3. Strain difference between healthy controls and the RhA patients : Box Plot showing no statistically significant difference between RhA patients and healthy controls for PALS. The figure shows wide variation in the Peak longitudinal strain for both groups specially the upper quartile. The lower quartile has narrow 95% confidence intervals and the median is almost overlapping, This trend would translate clinically into not much difference overall. However, the numbers are small to come to a definite conclusion. Nevertheless, the trend is clearly there to indicate higher strain in healthy individuals as compared to RhA patients and this trend may be more evident with higher sample size.

7.4 Discussion

7.4.1 Main Findings

This study has the main finding that using STE makes it feasible to study right atrial strain in inflammatory cardiomyopathies. Furthermore, right atrial strain is not decreased in RhA as compared to healthy controls, although there is a clear trend between two groups with RA Strain is being lower than the healthy controls.

To the best of our knowledge this is the first study of its kind exploring right atrial strain in rheumatic cardiomyopathies. Although RV systolic dysfunction[171] has been shown previously in a limited number of studies by various groups, there has been very limited emphasis on the right atrium and at best right atrial dilation has been reported in a limited number of studies.

Right atrial dysfunction can occur due to several etiologies. It has been reported that fibrinous pericarditis is present in 30 to 50% of patients with RhA and the firm attachment of fibrinous pericardium leading to adhesion formation could limit the movement of the right atrium, especially the most mobile lateral annular segment.

Fibrosis due to conversion of type three collagen to type one collagen leading to decreased tensile strength and elasticity of right atrial fibres may also contribute. Matrix metalloproteinase are the mediators of this process.

Right atrial dilation due to increased stretching due to high blood pressure, which is a co-morbidity of these diseases, leads to increased path length of atrial electrical wavelets, leading to altered electromechanical function and decreased mechanical activity. However, in the current study, strain in RhA patients was not different to that in the healthy population.

Chapter 8

Conclusions and Future Directions

8.1 Conclusions

From these experimental studies, we can conclude that STE is feasible for the study of right atrial phasic mechanics. The technique, originally designed for the left ventricle, can be applied to the right atrium and we now have defined normal reference ranges for the healthy population. HFnEF patients have lower longitudinal strain parameters for the right atrium as compared to the healthy controls. Strain in RhA patients is not much different to healthy controls.

In summary, the current series of experiments provides evidence that right atrial deformation study through speckle tracking echocardiography is possible, however, there are some technological challenges which lead to poor limits of agreement. Major technological advances in image acquisition and image analysis techniques are needed before right atrial speckle tracking can become a mainstream clinical practice. To the best of our knowledge, this is the first study of our kind which has addressed the important topic of standardizing the methodology of right atrial strain analysis through STE and more importantly validation of right atrial strain through STE. Although, the results of validation are not very encouraging , however, some important reasons have been brought forward which include but not limited to

1 When examining a specific chamber of the heart other than left ventricle , the images should be optimized for that particular chamber. This becomes all the more important for the right ventricle and the right atrium which can be visualized in the apical 4 chamber view but the speckle density , speckle distribution and speckle statistics can not be 100% accurate for RV or the right atrium because if the foucs is on the LV the lateral resolution of ultrasound waves is not really good. This can be overcome by 3 dimensional echocardiography but given the complex architechture of the right atrium, first statistical, biomechanical models and phantom studies need to be done before we can safely put our foot into realms of 3D atrial STE.

2 Getting the same standardized slice of the right atrium needs to be acquired each time in the same patient and different patients at different time points, because the right atrium has such a complex anatomy that slice position affects the endocardial definition. Therefore, the slice position needs to be defined and standardized

3 To get optimal image in a patient or healthy individual, the machine settings need to be defined. One such successful attempt has been made for 3 dimensional echocardiography for the right atrium, there is need that criterion needs to be defined for 2D transthoracic echocardiography as well.

Despite the limitations, we have successfully defined ranges for a mainly female cohort, which can be used as reference in future studies.

Additionally, the comparison of feature tracking CMR and STE has been done which showed poor agreement between the two techniques due to reasons discussed in detail previously in chapter 5.

Secondly we investigated the presence or absence of differences in deformation parameters between right atrial strain in HFNEF and RhA cohorts. HFNEF cohort

showed lower strain values during reservoir and conduit phase while the RhA patients did not show significant difference from normal controls. However there was a clear trend towards lower strain in the diseased group. This shows that despite less than optimal limits of agreement, STE can detect differences between healthy and diseased groups.

8.2 Future Directions

8.2.1 STE Image Quality and Strain

One of the most important parameters determining the accuracy of results appears to be image quality. Image quality may be subjectively defined in terms of the perceived degradation of the image in comparison to an ideal image. An objective definition has been a matter of much debate and several measures have been proposed, all of which have some strengths and weaknesses.[172, 173]

An important further study will be to elucidate the effect of image quality on speckle tracking-derived strain and other deformation parameters. This could be done by altering various parameters during the acquisition of echocardiographic images, which affect the speckle density, speckle shape, speckle intensity, and speckle distribution during acquisition, preprocessing, and post-processing. These parameters include but are not limited to frame rate, sector width, line density, time gain compensation, gain, depth, second harmonics, frequency, compressions and mechanical index to name a few.

By altering these in various combinations, it would be possible to determine the pattern of change in image quality.

8.2.2 Study of Right AV Mechanical Coupling

It would be interesting to study the right atrium and the right ventricle to study the interrelationship of the whole heart.

This is relevant in many clinical situations like primary and secondary pulmonary arterial hypertension, COPD, asthma, cystic fibrosis and other pulmonary diseases. So far only a limited number of studies have studied the RV function during systole and diastole in these diseases but the effect of altered RV preload (through the study of function of RA simultaneously. RV preload alterations alter the contractility by shifting the Frank–Starling curve. Additionally, right atrial flow is in continuity with right ventricular blood flow, and study of the blood vortices from the right atrium to ventricle has given insight into the functioning of the right side of the heart. A similar study on mechanical function may help to unravel the mystery even further. Now that feature tracking can be performed on MRI data in a similar way to STE, mechanical and flow function can be studied in a single patient at the same time, which can shed some light on how the human heart functions at the microscopic level.

RA function has been studied separately in PAH through STE.[84] Similarly, right ventricular function has been studied in some studies.[10, 105, 174-176] However, apart from the study by Boomer et al there is very limited data on right atrium and right ventricular structure and function simultaneously.

To address this question we could simply calculate the deformation indices of the right atrium and right ventricle in an apical four-chamber view, and measure the systolic and diastolic function indices of the right side of the heart such as the Tei index, TAPSE, tricuspid inflow velocities, TDI indices, ventricular size and volume and RAVI. We can

then explore how right atrial indices and RV indices vary in various disease states and in healthy individuals.

References

1. Quintana M, Lindell P, Saha S, del Furia F, Lind B, Govind S, Brodin L-A. Assessment of atrial regional and global electromechanical function by tissue velocity echocardiography: A feasibility study on healthy individuals. *Cardiovascular Ultrasound*. 2005;3:4
2. Ueda A, McCarthy KP, Sánchez-Quintana D, Yen Ho S. The right atrial appendage and vestibule: Further anatomical insights with implications for invasive electrophysiology. *Europace*. 2013;15:728-734
3. Kalman JM, Olgin JE, Karch MR, Hamdan M, Lee RJ, Lesh MD. "Cristal tachycardias": Origin of right atrial tachycardias from the crista terminalis identified by intracardiac echocardiography. *Journal of the American College of Cardiology*. 1998;31:451-459
4. Okumura Y, Watanabe I, Yamada T, Ohkubo K, Sugimura H, Hashimoto K, Kofune T, Takagi Y, Wakita RIE, Oshikawa N, Kawauchi K, Saito S, Ozawa Y, Kanmatsuse K, Yoshikawa Y, Asakawa Y. Relationship between anatomic location of the crista terminalis and double potentials recorded during atrial flutter. *Journal of Cardiovascular Electrophysiology*. 2004;15:1426-1432
5. Aslanidi OV, Boyett MR, Dobrzynski H, Li J, Zhang H. Mechanisms of transition from normal to reentrant electrical activity in a model of rabbit atrial tissue: Interaction of tissue heterogeneity and anisotropy. *Biophysical Journal*. 2009;96:798-817
6. Gaynor SL, Maniar HS, Prasad SM, Steendijk P, Moon MR. Reservoir and conduit function of the right atrium: Impact on the right ventricular filling and cardiac output. *American Journal of Physiology - Heart and Circulatory Physiology*. 2005;288:H2140-H2145
7. Barbier P, Solomon S, Shiller N, Glantz S. Left atrial relaxation and left ventricular systolic function determine left atrial reservoir function. *Circulation*. 1999;100:427 - 436
8. Grant C, Bunnell IL, Greene DG. The reservoir function of the left atrium during ventricular systole: An angiocardiographic study of atrial stroke volume and work. *The American journal of medicine*. 1964;37:36-43
9. Spencer KT, Mor-Avi V, Gorcsan J, DeMaria AN, Kimball TR, Monaghan MJ, Perez JE, Weinert L, Bednarz J, Edelman K, Kwan OL, Glascock B, Hancock J, Baumann C, Lang RM. Effects of aging on left atrial reservoir, conduit, and booster pump function: A multi-institution acoustic quantification study. *Heart*. 2001;85:272-277
10. Bommer W, Weinert L, Neumann A, Neef J, Mason DT, DeMaria A. Determination of the right atrial and the right ventricular size by two-dimensional echocardiography. *Circulation*. 1979;60:91-100
11. Keller A, Gopal A, King D. Left and the right atrial volume by freehand three-dimensional echocardiography: In vivo validation using magnetic resonance imaging. *Eur J Echocardiogr*. 2000;1:55 - 65
12. Schabelman S, Schiller NB, Silverman NH, Ports TA. Left atrial volume estimation by two-dimensional echocardiography. *Catheterization and Cardiovascular Diagnosis*. 1981;7:165-178
13. Koka AR, Yau J, Van Why C, Cohen IS, Halpern EJ. Underestimation of left atrial size measured with transthoracic echocardiography compared with 3d mdct. *American Journal of Roentgenology*. 2010;194:W375-W381

14. Faletra FF, Ho SY, Auricchio A. Anatomy of the right atrial structures by real-time 3d transesophageal echocardiography. *J Am Coll Cardiol Img*. 2010;3:966-975
15. Castello R, Pearson AC, Labovitz AJ. Prevalence and clinical implications of atrial spontaneous contrast in patients undergoing transesophageal echocardiography. *The American Journal of Cardiology*. 1990;65:1149-1153
16. Akoum N, McGann C, Vergara G, Badger T, Ranjan R, Mahnkopf C, Kholmovski E, Macleod ROB, Marrouche N. Atrial fibrosis quantified using late gadolinium enhancement mri is associated with sinus node dysfunction requiring pacemaker implant. *Journal of Cardiovascular Electrophysiology*. 2012;23:44-50
17. Ozgun M, Kirchhof P, Bunck AC, Heindel W, Eckardt L, Maintz D. Mri of the right atrial function after catheter ablation of atrial flutter. *Academic Radiology*. 2010;17:856-861
18. Fleck T, Wolf F, Bader T, Lehner R, Aigner C, Stix G, Wolner E, Wisser W. Atrial function after ablation procedure in patients with chronic atrial fibrillation using steady-state free precession magnetic resonance imaging. *The Annals of Thoracic Surgery*. 2007;84:1600-1604
19. Gade C, Bergman G, Naidu S, Weinsaft J, Callister T, Min J. Comprehensive evaluation of atrial septal defects in individuals undergoing percutaneous repair by 64-detector row computed tomography. *The International Journal of Cardiovascular Imaging (formerly Cardiac Imaging)*. 2007;23:397-404
20. McDonald IG. The shape and movements of the human left ventricle during systole: A study by cineangiography and by cineradiography of epicardial markers. *The American Journal of Cardiology*. 1970;26:221-230
21. POMBO JF, TROY BL, RUSSELL RO. Left ventricular volumes and ejection fraction by echocardiography. *Circulation*. 1971;43:480-490
22. Fouad FM, Slominski JM, Tarazi RC. Left ventricular diastolic function in hypertension: Relation to left ventricular mass and systolic function. *Journal of the American College of Cardiology*. 1984;3:1500-1506
23. Kass DA, Maughan WL, Guo ZM, Kono A, Sunagawa K, Sagawa K. Comparative influence of load versus inotropic states on indexes of ventricular contractility: Experimental and theoretical analysis based on pressure-volume relationships. *Circulation*. 1987;76:1422-1436
24. Gaasch WH, Little WC. Assessment of left ventricular diastolic function and recognition of diastolic heart failure. *Circulation*. 2007;116:591-593
25. MASON DT, BRAUNWALD E, COVELL JW, SONNENBLICK EH, ROSS J. Assessment of cardiac contractility: The relation between the rate of pressure rise and ventricular pressure during isovolumic systole. *Circulation*. 1971;44:47-58
26. Urheim S, Edvardsen T, Torp H, Angelsen B, Smiseth OA. Myocardial strain by doppler echocardiography. *Circulation*. 2000;102:1158-1164
27. Greenberg NL, Firstenberg MS, Castro PL, Main M, Travaglini A, Odabashian JA, Drinko JK, Rodriguez LL, Thomas JD, Garcia MJ. Doppler-derived myocardial systolic strain rate is a strong index of left ventricular contractility. *Circulation*. 2002;105:99-105
28. Amundsen BH, Helle-Valle T, Edvardsen T, Torp H, Crosby J, Lyseggen E, Støylen A, Ihlen H, Lima JAC, Smiseth OA, Slørdahl SA. Noninvasive myocardial strain measurement by speckle tracking echocardiography:

Validation against sonomicrometry and tagged magnetic resonance imaging. *Journal of the American College of Cardiology*. 2006;47:789-793
29. Helle-Valle T, Crosby J, Edvardsen T, Lyseggen E, Amundsen BH, Smith H-J, Rosen BD, Lima JAC, Torp H, Ihlen H, Smiseth OA. New noninvasive method for assessment of left ventricular rotation. *Circulation*. 2005;112:3149-3156
30. Rappaport D, Adam D, Lysyansky P, Riesner S. Assessment of myocardial regional strain and strain rate by tissue tracking in b-mode echocardiograms. *Ultrasound in Medicine & Biology*. 2006;32:1181-1192
31. Behar V, Adam D, Lysyansky P, Friedman Z. The combined effect of nonlinear filtration and window size on the accuracy of tissue displacement estimation using detected echo signals. *Ultrasonics*. 2004;41:743-753
32. Geyer H, Caracciolo G, Abe H, Wilansky S, Carerj S, Gentile F, Nesser H-J, Khandheria B, Narula J, Sengupta PP. Assessment of myocardial mechanics using speckle tracking echocardiography: Fundamentals and clinical applications. *Journal of the American Society of Echocardiography*. 2010;23:351-369
33. Marwick TH. Measurement of strain and strain rate by echocardiography: Ready for prime time? *J Am Coll Cardiol*. 2006;47:1313-1327
34. Edvardsen T, Gerber BL, Garot J, Bluemke DA, Lima JAC, Smiseth OA. Quantitative assessment of intrinsic regional myocardial deformation by doppler strain rate echocardiography in humans. *Circulation*. 2002;106:50-56
35. Nesser H-J, Mor-Avi V, Gorissen W, Weinert L, Steringer-Mascherbauer R, Niel J, Sugeng L, Lang RM. Quantification of left ventricular volumes using three-dimensional echocardiographic speckle tracking: Comparison with mri. *European Heart Journal*. 2009;30:1565-1573
36. Mondillo S, Galderisi M, Mele D, Cameli M, Lomoriello VS, Zaca V, Ballo P, D'Andrea A, Muraru D, Losi M, Agricola E, D'Errico A, Buralli S, Sciomer S, Nistri S, Badano L. Speckle-tracking echocardiography: A new technique for assessing myocardial function. *J Ultrasound Med*. 2011;30:71-83
37. Notomi Y, Lysyansky P, Setser RM, Shiota T, Popović ZB, Martin-Miklovic MG, Weaver JA, Oryszak SJ, Greenberg NL, White RD, Thomas JD. Measurement of ventricular torsion by two-dimensional ultrasound speckle tracking imaging. *Journal of the American College of Cardiology*. 2005;45:2034-2041
38. Congxian J, Olafsson R, Sheng-Wen H, Kolias TJ, Kang K, Rubin JM, Hua X, O'Donnell M. Comparison of 2-d speckle tracking and tissue doppler imaging in an isolated rabbit heart model. *Ultrasonics, Ferroelectrics and Frequency Control, IEEE Transactions on*. 2010;57:2491-2502
39. Burckhardt CB. Speckle in ultrasound b-mode scans. *Sonics and Ultrasonics, IEEE Transactions on*. 1978;25:1-6
40. Blessberger H, Binder T. Non-invasive imaging: Two dimensional speckle tracking echocardiography: Basic principles. *Heart*. 2010;96:716-722
41. Sengupta PP, Tajik AJ, Chandrasekaran K, Khandheria BK. Twist mechanics of the left ventricle: Principles and application. *JACC Cardiovasc Imaging*. 2008;1:366-376
42. Wang J, Khoury DS, Yue Y, Torre-Amione G, Nagueh SF. Left ventricular untwisting rate by speckle tracking echocardiography. *Circulation*. 2007;116:2580-2586

43. Notomi Y, Martin-Miklovic MG, Oryszak SJ, Shiota T, Deserranno D, Popovic ZB, Garcia MJ, Greenberg NL, Thomas JD. Enhanced ventricular untwisting during exercise. *Circulation*. 2006;113:2524-2533
44. Shivu GN, Abozguia K, Phan TT, Narendran P, Stevens M, Frenneaux M. Left ventricular filling patterns and its relation to left ventricular untwist in patients with type 1 diabetes and normal ejection fraction. *International Journal of Cardiology*.
45. Haggerty C, Kramer S, Binkley C, Powell D, Mattingly A, Charnigo R, Epstein F, Fornwalt B. Reproducibility of cine displacement encoding with stimulated echoes (dense) cardiovascular magnetic resonance for measuring left ventricular strains, torsion, and synchrony in mice. *Journal of Cardiovascular Magnetic Resonance*. 2013;15:71
46. Awtry EH, Davidoff R. Low-flow low-gradient aortic stenosis. *Circulation: Cardiovascular Imaging*. 2012;5:6-8
47. Takeuchi M, Borden WB, Nakai H, Nishikage T, Kokumai M, Nagakura T, Otani S, Lang RM. Reduced and delayed untwisting of the left ventricle in patients with hypertension and left ventricular hypertrophy: A study using two-dimensional speckle tracking imaging. *European Heart Journal*. 2007;28:2756-2762
48. Kosmala W, Plaksej R, Strotmann JM, Weigel C, Herrmann S, Niemann M, Mende H, Störk S, Angermann CE, Wagner JA, Weidemann F. Progression of left ventricular functional abnormalities in hypertensive patients with heart failure: An ultrasonic two-dimensional speckle tracking study. *Journal of the American Society of Echocardiography*. 2008;21:1309-1317
49. Ernande L, Rietzschel ER, Bergerot C, De Buyzere ML, Schnell F, Groisne L, Ovize M, Croisille P, Moulin P, Gillebert TC, Derumeaux G. Impaired myocardial radial function in asymptomatic patients with type 2 diabetes mellitus: A speckle-tracking imaging study. *Journal of the American Society of Echocardiography*. 2010;23:1266-1272
50. Ng ACT, Delgado V, Bertini M, van der Meer RW, Rijzewijk LJ, Shanks M, Nucifora G, Smit JWA, Diamant M, Romijn JA, de Roos A, Leung DY, Lamb HJ, Bax JJ. Findings from left ventricular strain and strain rate imaging in asymptomatic patients with type 2 diabetes mellitus. *The American Journal of Cardiology*. 2009;104:1398-1401
51. Langeland S, D'hooge J, Wouters PF, Leather HA, Claus P, Bijnens B, Sutherland GR. Experimental validation of a new ultrasound method for the simultaneous assessment of radial and longitudinal myocardial deformation independent of insonation angle. *Circulation*. 2005;112:2157-2162
52. Jones CJ, Raposo L, Gibson DG. Functional importance of the long axis dynamics of the human left ventricle. *British Heart Journal*. 1990;63:215-220
53. Shivu GN, Abozguia K, Phan TT, Ahmed I, Weaver R, Narendran P, Stevens M, Frenneaux M. Increased left ventricular torsion in uncomplicated type 1 diabetic patients. *Diabetes Care*. 2009;32:1710-1712
54. Chung J, Abraszewski P, Yu X, Liu W, Krainik AJ, Ashford M, Caruthers SD, McGill JB, Wickline SA. Paradoxical increase in ventricular torsion and systolic torsion rate in type i diabetic patients under tight glycemic control. *Journal of the American College of Cardiology*. 2006;47:384-390
55. Wigle ED, Rakowski H, Kimball BP, Williams WG. Hypertrophic cardiomyopathy. *Circulation*. 1995;92:1680-1692

56. Serri K, Reant P, Lafitte M, Berhouet M, Le Bouffos V, Roudaut R, Lafitte S. Global and regional myocardial function quantification by two-dimensional strain: Application in hypertrophic cardiomyopathy. *Journal of the American College of Cardiology*. 2006;47:1175-1181
57. Paraskevaidis IA, Panou F, Papadopoulos C, Farmakis D, Parissis J, Ikonomidis I, Rigopoulos A, Iliodromitis EK, Th Kremastinos D. Evaluation of left atrial longitudinal function in patients with hypertrophic cardiomyopathy: A tissue doppler imaging and two-dimensional strain study. *Heart*. 2009;95:483-489
58. Christian Prinz HE, Wolfgang Burchert, Dieter Horstkotte, Lothar Faber, Heart- and Diabetes Center NRW, Bad Oeynhausen. In patients with hypertrophic cardiomyopathy myocardial fibrosis is associated withleft ventricular and left atrial dysfunction. *journal of american college of cardiology*. 2011;57
59. Prinz C, van Buuren F, Faber L, Bitter T, Bogunovic N, Burchert W, Horstkotte D. Myocardial fibrosis is associated with biventricular dysfunction in patients with hypertrophic cardiomyopathy. *Echocardiography*. 2012;29:438-444
60. Saito M, Okayama H, Nishimura K, Ogimoto A, Ohtsuka T, Inoue K, Hiasa G, Sumimoto T, Funada J, Shigematsu Y, Higaki J. Determinants of left ventricular untwisting behaviour in patients with dilated cardiomyopathy: Analysis by two-dimensional speckle tracking. *Heart*. 2009;95:290-296
61. Matsumoto K, Tanaka H, Tatsumi K, Miyoshi T, Hiraishi M, Kaneko A, Tsuji T, Ryo K, Fukuda Y, Yoshida A, Kawai H, Hirata K-I. Left ventricular dyssynchrony using three-dimensional speckle-tracking imaging as a determinant of torsional mechanics in patients with idiopathic dilated cardiomyopathy. *The American Journal of Cardiology*. 2012;109:1197-1205
62. Sengupta PP, Krishnamoorthy VK, Abhayaratna WP, Korinek J, Belohlavek M, Sundt Iii TM, Chandrasekaran K, Mookadam F, Seward JB, Tajik AJ, Khandheria BK. Disparate patterns of left ventricular mechanics differentiate constrictive pericarditis from restrictive cardiomyopathy. *JACC: Cardiovascular Imaging*. 2008;1:29-38
63. Sitia S, Tomasoni L, Cicala S, Atzeni F, Ricci C, Gaeta M, Sarzi-Puttini P, Turiel M. Detection of preclinical impairment of myocardial function in Rheumatoid Arthritis patients with short disease duration by speckle tracking echocardiography. *International Journal of Cardiology*. 2012;160:8-14
64. Fine NM, Crowson CS, Lin G, Oh JK, Villarraga HR, Gabriel SE. Evaluation of myocardial function in patients with Rheumatoid Arthritis using strain imaging by speckle-tracking echocardiography. *Annals of the Rheumatic Diseases*. 2013
65. Ikonomidis I, Tzortzis S, Lekakis J, Paraskevaidis I, Andreadou I, Nikolaou M, Kaplanoglou T, Katsimbri P, Skarantavos G, Soucacos P, Kremastinos DT. Lowering interleukin-1 activity with anakinra improves myocardial deformation in Rheumatoid Arthritis. *Heart*. 2009;95:1502-1507
66. Mansencal N, Abbou N, Pillière R, El Mahmoud R, Farcot J-C, Dubourg O. Usefulness of two-dimensional speckle tracking echocardiography for assessment of tako-tsubo cardiomyopathy. *The American Journal of Cardiology*. 2009;103:1020-1024
67. Lafitte S, Perlant M, Reant P, Serri K, Douard H, DeMaria A, Roudaut R. Impact of impaired myocardial deformations on exercise tolerance and prognosis in patients with asymptomatic aortic stenosis. *European Journal of Echocardiography*. 2009;10:414-419

68. Becker M, Kramann R, Dohmen G, Lückhoff A, Autschbach R, Kelm M, Hoffmann R. Impact of left ventricular loading conditions on myocardial deformation parameters: Analysis of early and late changes of myocardial deformation parameters after aortic valve replacement. *Journal of the American Society of Echocardiography*. 2007;20:681-689
69. Kearney LG, Lu K, Ord M, Patel SK, Profitis K, Matalanis G, Burrell LM, Srivastava PM. Global longitudinal strain is a strong independent predictor of all-cause mortality in patients with aortic stenosis. *European Heart Journal – Cardiovascular Imaging*. 2012;13:827-833
70. Olsen NT, Sogaard P, Larsson HB, Goetze JP, Jons C, Mogelvang R, Nielsen OW, Fritz-Hansen T. Speckle-tracking echocardiography for predicting outcome in chronic aortic regurgitation during conservative management and after surgery. *JACC Cardiovasc Imaging*. 2011;4:223-230
71. Borg AN, Harrison JL, Argyle RA, Ray SG. Left ventricular torsion in primary chronic mitral regurgitation. *Heart*. 2008;94:597-603
72. Yilmaz A, Sechtem U. Cardiac involvement in muscular dystrophy: Advances in diagnosis and therapy. *Heart*. 2012;98:420-429
73. Abdulrahman RM, Delgado V, Ng ACT, Ewe SH, Bertini M, Holman ER, Hovens GC, Pereira AM, Romijn JA, Bax JJ, Smit JW. Abnormal cardiac contractility in long-term exogenous subclinical hyperthyroid patients as demonstrated by two-dimensional echocardiography speckle tracking imaging. *European Journal of Endocrinology*. 2010;163:435-441
74. Germanakis I, Matsui H, Gardiner HM. Myocardial strain abnormalities in fetal congenital heart disease assessed by speckle tracking echocardiography. *Fetal Diagnosis and Therapy*. 2012;32:123-130
75. Suffoletto MS, Dohi K, Cannesson M, Saba S, Gorcsan J. Novel speckle-tracking radial strain from routine black-and-white echocardiographic images to quantify dyssynchrony and predict response to cardiac resynchronization therapy. *Circulation*. 2006;113:960-968
76. Delgado V, Bax JJ. Assessment of systolic dyssynchrony for cardiac resynchronization therapy is clinically useful / response to delgado and bax. *Circulation*. 2011;123:640-655
77. Esch BT, Scott JM, Warburton DER, Thompson R, Taylor D, Baron JC, Paterson I, Haykowsky MJ. Left ventricular torsion and untwisting during exercise in heart transplant recipients. *The Journal of Physiology*. 2009;587:2375-2386
78. Pirat B, McCulloch ML, Zoghbi WA. Evaluation of global and regional the right ventricular systolic function in patients with pulmonary hypertension using a novel speckle tracking method. *The American Journal of Cardiology*. 2006;98:699-704
79. Vianna-Pinton R, Moreno C, Baxter C, Lee K, Tsang T, Appleton C. Two-dimensional speckle-tracking echocardiography of the the Right atrium: Feasibility and regional contraction and relaxation differences in normal subjects. *J Am Soc Echocardiogr*. 2009;22:299 - 305
80. Schneider C, Malisius R, Krause K, Lampe F, Bahlmann E, Boczor S, Antz M, Ernst S, Kuck K-H. Strain rate imaging for functional quantification of the the Right atrium: Atrial deformation predicts the maintenance of sinus rhythm after catheter ablation of atrial fibrillation. *European Heart Journal*. 2008;29:1397-1409

81. Inaba Y, Yuda S, Kobayashi N, Hashimoto A, Uno K, Nakata T, Tsuchihashi K, Miura T, Ura N, Shimamoto K. Strain rate imaging for noninvasive functional quantification of the the Right atrium: Comparative studies in controls and patients with atrial fibrillation. *J Am Soc Echocardiogr*. 2005;18:729 - 736
82. Saraiva RM, Demirkol S, Buakhamsri A, Greenberg N, Popović ZB, Thomas JD, Klein AL. Left atrial strain measured by two-dimensional speckle tracking represents a new tool to evaluate left atrial function. *Journal of the American Society of Echocardiography*. 2010;23:172-180
83. Cameli M, Lisi M, Mondillo S, Padeletti M, Ballo P, Tsioulpas C, Bernazzali S, Maccherini M. Left atrial longitudinal strain by speckle tracking echocardiography correlates well with left ventricular filling pressures in patients with heart failure. *Cardiovascular Ultrasound*. 2010;8:14
84. Padeletti M, Cameli M, Lisi M, Malandrino A, Zacà V, Mondillo S. Reference values of the right atrial longitudinal strain imaging by two-dimensional speckle tracking. *Echocardiography*. 2012;29:147-152
85. D'Andrea A, Scarafile R, Riegler L, Salerno G, Gravino R, Cocchia R, Castaldo F, Allocca F, Limongelli G, Di Salvo G, Cuomo S, Pacileo G, Caso P, Russo MG, Calabrò R. Right atrial size and deformation in patients with dilated cardiomyopathy undergoing cardiac resynchronization therapy. *European Journal of Heart Failure*. 2009;11:1169-1177
86. Sileikiene R, Vaskelyte J, Mizariene V, Nedzelskiene I, Verseckaite R, Jurkevicius R, Baksiene D, Sileikyte V, Kevalas R. Heart rate variability and atria function in children at late follow-up evaluation after atrioventricular node slow-pathway radiofrequency ablation. *Pediatr Cardiol*. 2011;32:792-800
87. Schueler R, Sinning J-M, Momcilovic D, Weber M, Ghanem A, Werner N, Nickenig G, Grube E, Hammerstingl C. Three-dimensional speckle-tracking analysis of left ventricular function after transcatheter aortic valve implantation. *Journal of the American Society of Echocardiography*. 2012;25:827-834.e821
88. Leung DY, Ng AC. Emerging clinical role of strain imaging in echocardiography. *Heart Lung Circ*. 2010;19:161-174
89. Oxborough D, George K, Birch KM. Intraobserver reliability of two-dimensional ultrasound derived strain imaging in the assessment of the left ventricle, the right ventricle, and the left atrium of healthy human hearts. *Echocardiography*. 2012:no-no
90. Kuppahally SS, Akoum N, Badger TJ, Burgon NS, Haslam T, Kholmovski E, Macleod R, McGann C, Marrouche NF. Echocardiographic left atrial reverse remodeling after catheter ablation of atrial fibrillation is predicted by preablation delayed enhancement of the left atrium by magnetic resonance imaging. *American Heart Journal*. 2010;160:877-884
91. Dalen H, Thorstensen A, Aase SA, Ingul CB, Torp H, Vatten LJ, Stoylen A. Segmental and global longitudinal strain and strain rate based on echocardiography of 1266 healthy individuals: The hunt study in norway. *European Journal of Echocardiography*. 2010;11:176-183
92. Choi J-O, Shin D-H, Cho SW, Song YB, Kim JH, Kim YG, Lee S-C, Park SW. Effect of preload on left ventricular longitudinal strain by 2d speckle tracking. *Echocardiography*. 2008;25:873-879
93. Gayat E, Ahmad H, Weinert L, Lang RM, Mor-Avi V. Reproducibility and inter-vendor variability of left ventricular deformation measurements by three-dimensional speckle-tracking echocardiography. *Journal of the American*

Society of Echocardiography : official publication of the American Society of Echocardiography. 2011;24:878-885
94. Cameli M, Caputo M, Mondillo S, Ballo P, Palmerini E, Lisi M, Marino E, Galderisi M. Feasibility and reference values of left atrial longitudinal strain imaging by two-dimensional speckle tracking. *Cardiovascular Ultrasound*. 2009;7:6
95. Cameli M, Lisi M, Giacomin E, Caputo M, Navarri R, Malandrino A, Ballo P, Agricola E, Mondillo S. Chronic mitral regurgitation: Left atrial deformation analysis by two-dimensional speckle tracking echocardiography. *Echocardiography*. 2011;28:327 - 334
96. Cameli M, Lisi M, Righini F, Ballo P, Henein M, Mondillo S. Early detection of left atrial dysfunction in patients with hypertension by two-dimensional speckle tracking echocardiography. (abstr)in: Euroecho congress. Copenaghen 2010. *Eur J Echocardiogr, Abstracts Supplement*. 2010:P802
97. Mirza M, Jiamsripong P, Belohlavek M, Lanza L, Arabia F, Shen W-K, Jahangir A. Atrial mechanical abnormalities on speckle tracking echocardiography correlate with degree of fibrosis in patients with atrial fibrillation. *J Am Coll Cardiol*. 2012;59:E1559-
98. Reisner SA, Lysyansky P, Agmon Y, Mutlak D, Lessick J, Friedman Z. Global longitudinal strain: A novel index of left ventricular systolic function. *Journal of the American Society of Echocardiography : official publication of the American Society of Echocardiography*. 2004;17:630-633
99. Manning WJ, Katz SE, Douglas PS, Silverman DI. Atrial ejection force: A noninvasive assessment of atrial systolic function. *Journal of the American College of Cardiology*. 1993;22:221-225
100. Yingchoncharoen T, Agarwal S, Popović ZB, Marwick TH. Normal ranges of left ventricular strain: A meta-analysis. *Journal of the American Society of Echocardiography*. 2013;26:185-191
101. Casaclang-Verzosa G, Gersh BJ, Tsang TSM. Structural and functional remodeling of left atriumclinical and therapeutic implications for atrial fibrillation. *Journal of the American College of Cardiology*. 2008;51:1-11
102. Nattel S. Atrial electrophysiology and mechanisms of atrial fibrillation. *Journal of Cardiovascular Pharmacology and Therapeutics*. 2003;8:S5-S11
103. Padeletti M, Cameli M, Lisi M, Zaca V, Tsioulpas C, Bernazzali S, Maccherini M, Mondillo S. Right atrial speckle tracking analysis as a novel noninvasive method for pulmonary hemodynamics assessment in patients with chronic systolic heart failure. *Echocardiography*. 2011;28:658-664
104. Abadi S, Roguin A, Engel A, Lessick J. Feasibility of automatic assessment of four-chamber cardiac function with mdct: Initial clinical application and validation. *European Journal of Radiology*. 2010;74:175-181
105. Ocak I, Fuhrman C. Ct angiography findings of the left atrium and right ventricle in patients with massive pulmonary embolism. *American Journal of Roentgenology*. 2008;191:1072-1076
106. McKay T, Thomas L. Prominent crista terminalis and eustachian ridge in the right atrium: Two dimensional (2d) and three dimensional (3d) imaging. *European Journal of Echocardiography*. 2007;8:288-291
107. Anwar A, Soliman O, Geleijnse M, Nemes A, Vletter W, tenCate F. Assessment of left atrial volume and function by real-time three-dimensional echocardiography. *Int J Cardiol*. 2008;123:155 - 161

108. Rodevan O, Bjornerheim R, Ljosland M, Maehle J, Smith H, Ihlen H. Left atrial volumes assessed by three- and two-dimensional echocardiography compared to mri estimates. *Int J Card Imaging*. 1999;15:397 - 410
109. Bangalore S, Yao S-S, Chaudhry FA. Role of left atrial size in risk stratification and prognosis of patients undergoing stress echocardiography. *J Am Coll Cardiol*. 2007;50:1254-1262
110. Amparo E, Higgins C, Farmer D, Gamsu G, McNamara M. Gated mri of cardiac and paracardiac masses: Initial experience. *American Journal of Roentgenology*. 1984;143:1151-1156
111. Attili AK, Gebker R, Cascade PN. Radiological reasoning: Right atrial mass. *American Journal of Roentgenology*. 2007;188:S26-S30
112. Daccarett M, McGann CJ, Akoum NW, MacLeod RS, Marrouche NF. Mri of the the left atrium: Predicting clinical outcomes in patients with atrial fibrillation. *Expert Review of Cardiovascular Therapy*. 2010;9:105-111
113. Kuppahally S, Akoum N, Burgon N, Badger T, Kholmovski E, Vijayakumar S, Rao S, Blauer J, Fish E, Dibella E, Macleod R, McGann C, Litwin S, Marrouche N. Left atrial strain and strain rate in patients with paroxysmal and persistent atrial fibrillation: Relationship to left atrial structural remodeling detected by delayed-enhancement mri. *Circ Cardiovasc Imaging*. 2010;3:231 - 239
114. Hudsmith LE, Petersen SE, Francis JM, Robson MD, Neubauer S. Normal human left and right ventricular and left atrial dimensions using steady state free precession magnetic resonance imaging. *Journal of Cardiovascular Magnetic Resonance*. 2005;7:775-782
115. Augustine D, Lewandowski A, Lazdam M, Rai A, Francis J, Myerson S, Noble A, Becher H, Neubauer S, Petersen S, Leeson P. Global and regional left ventricular myocardial deformation measures by magnetic resonance feature tracking in healthy volunteers: Comparison with tagging and relevance of gender. *Journal of Cardiovascular Magnetic Resonance*. 2013;15:8
116. Angelini ED, Gerard O. Review of myocardial motion estimation methods from optical flow tracking on ultrasound data. *Engineering in Medicine and Biology Society, 2006. EMBS '06. 28th Annual International Conference of the IEEE*. 2006:1537-1540
117. Hor KN, Gottliebson WM, Carson C, Wash E, Cnota J, Fleck R, Wansapura J, Klimeczek P, Al-Khalidi HR, Chung ES, Benson DW, Mazur W. Comparison of magnetic resonance feature tracking for strain calculation with harmonic phase imaging analysis. *JACC: Cardiovascular Imaging*. 2010;3:144-151
118. Schuster A, Kutty S, Padiyath A, Parish V, Gribben P, Danford D, Makowski M, Bigalke B, Beerbaum P, Nagel E. Cardiovascular magnetic resonance myocardial feature tracking detects quantitative wall motion during dobutamine stress. *Journal of Cardiovascular Magnetic Resonance*. 2011;13:58
119. Osman N, Prince J. Regenerating mr tagged images using harmonic phase (harp) methods. *IEEE Trans Biomed Eng*. 2004;51:1428 - 1433
120. Osman NF, Kerwin WS, McVeigh ER, Prince JL. Cardiac motion tracking using cine harmonic phase (harp) magnetic resonance imaging. *Magnetic Resonance in Medicine*. 1999;42:1048-1060
121. Hess AT, Zhong X, Spottiswoode BS, Epstein FH, Meintjes EM. Myocardial 3d strain calculation by combining cine displacement encoding with stimulated echoes (dense) and cine strain encoding (senc) imaging. *Magnetic Resonance in Medicine*. 2009;62:77-84

122. Ibrahim E-S. Myocardial tagging by cardiovascular magnetic resonance: Evolution of techniques--pulse sequences, analysis algorithms, and applications. *Journal of Cardiovascular Magnetic Resonance*. 2011;13:36
123. O'Dell WG, Moore CC, Hunter WC, Zerhouni EA, McVeigh ER. Three-dimensional myocardial deformations: Calculation with displacement field fitting to tagged mr images. *Radiology*. 1995;195:829-835
124. Maret E, Todt T, Brudin L, Nylander E, Swahn E, Ohlsson J, Engvall J. Functional measurements based on feature tracking of cine magnetic resonance images identify left ventricular segments with myocardial scar. *Cardiovascular Ultrasound*. 2009;7:53
125. Members WG, Roger VL, Go AS, Lloyd-Jones DM, Benjamin EJ, Berry JD, Borden WB, Bravata DM, Dai S, Ford ES, Fox CS, Fullerton HJ, Gillespie C, Hailpern SM, Heit JA, Howard VJ, Kissela BM, Kittner SJ, Lackland DT, Lichtman JH, Lisabeth LD, Makuc DM, Marcus GM, Marelli A, Matchar DB, Moy CS, Mozaffarian D, Mussolino ME, Nichol G, Paynter NP, Soliman EZ, Sorlie PD, Sotoodehnia N, Turan TN, Virani SS, Wong ND, Woo D, Turner MB. Heart disease and stroke statistics—2012 update: A report from the american heart association. *Circulation*. 2012;125:e2-e220
126. Owan TE, Hodge DO, Herges RM, Jacobsen SJ, Roger VL, Redfield MM. Trends in prevalence and outcome of heart failure with preserved ejection fraction. *New England Journal of Medicine*. 2006;355:251-259
127. Lee DS, Gona P, Vasan RS, Larson MG, Benjamin EJ, Wang TJ, Tu JV, Levy D. Relation of disease pathogenesis and risk factors to heart failure with preserved or reduced ejection fraction: Insights from the framingham heart study of the national heart, lung, and blood institute. *Circulation*. 2009;119:3070-3077
128. Benjamin EJ, D'Agostino RB, Belanger AJ, Wolf PA, Levy D. Left atrial size and the risk of stroke and death. The framingham heart study. *Circulation*. 1995;92:835-841
129. Maeder MT, Kaye DM. Heart failure with normal left ventricular ejection fraction. *Journal of the American College of Cardiology*. 2009;53:905-918
130. Tan YT, Wenzelburger FW, Sanderson JE, Leyva F. Exercise-induced torsional dyssynchrony relates to impaired functional capacity in patients with heart failure and normal ejection fraction. *Heart*. 2013;99:259-266
131. Neubauer S. The failing heart — an engine out of fuel. *New England Journal of Medicine*. 2007;356:1140-1151
132. Neubauer S, Horn M, Cramer M, Harre K, Newell JB, Peters W, Pabst T, Ertl G, Hahn D, Ingwall JS, Kochsiek K. Myocardial phosphocreatine-to-atp ratio is a predictor of mortality in patients with dilated cardiomyopathy. *Circulation*. 1997;96:2190-2196
133. Yu C-M, Lin H, Zhang Q, Sanderson JE. High prevalence of left ventricular systolic and diastolic asynchrony in patients with congestive heart failure and normal qrs duration. *Heart*. 2003;89:54-60
134. Carlhäll CJ, Bolger A. Passing strange: Flow in the failing ventricle. *Circulation: Heart Failure*. 2010;3:326-331
135. Aurigemma GP, Gaasch WH. Diastolic heart failure. *New England Journal of Medicine*. 2004;351:1097-1105
136. Baicu CF, Zile MR, Aurigemma GP, Gaasch WH. Left ventricular systolic performance, function, and contractility in patients with diastolic heart failure. *Circulation*. 2005;111:2306-2312

137. Bellenger NG, Burgess MI, Ray SG, Lahiri A, Coats AJS, Cleland JGF, Pennell DJ. Comparison of left ventricular ejection fraction and volumes in heart failure by echocardiography, radionuclide ventriculography and cardiovascular magnetic resonance. Are they interchangeable? *European Heart Journal*. 2000;21:1387-1396
138. Bhella PS, Pacini EL, Prasad A, Hastings JL, Adams-Huet B, Thomas JD, Grayburn PA, Levine BD. Echocardiographic indices do not reliably track changes in left-sided filling pressure in healthy subjects or patients with heart failure with preserved ejection fraction. *Circulation: Cardiovascular Imaging*. 2011;4:482-489
139. Cameli M, Lisi M, Mondillo S, Padeletti M, Ballo P, Tsioulpas C, Bernazzali S, Maccherini M. Left atrial longitudinal strain by speckle tracking echocardiography correlates well with left ventricular filling pressures in patients with heart failure. *Cardiovasc Ultrasound*. 2010;8:14
140. Drazner MH, Prasad A, Ayers C, Markham DW, Hastings J, Bhella PS, Shibata S, Levine BD. The relationship of right- and left-sided filling pressures in patients with heart failure and a preserved ejection fraction. *Circulation: Heart Failure*. 2010;3:202-206
141. Edvardsen T, Helle-Valle T, Smiseth OA. Systolic dysfunction in heart failure with normal ejection fraction: Speckle-tracking echocardiography. *Progress in Cardiovascular Diseases*. 2006;49:207-214
142. Gharib M, Rambod E, Kheradvar A, Sahn DJ, Dabiri JO. Optimal vortex formation as an index of cardiac health. *Proceedings of the National Academy of Sciences*. 2006;103:6305-6308
143. Hoit BD, Shao Y, Gabel M, Walsh RA. Left atrial mechanical and biochemical adaptation to pacing induced heart failure. *Cardiovascular Research*. 1995;29:469-474
144. Kindermann M, Reil J-C, Pieske B, van Veldhuisen DJ, Böhm M. Heart failure with normal left ventricular ejection fraction: What is the evidence? *Trends in Cardiovascular Medicine*. 2008;18:280-292
145. Li D, Shinagawa K, Pang L, Leung TK, Cardin S, Wang Z, Nattel S. Effects of angiotensin-converting enzyme inhibition on the development of the atrial fibrillation substrate in dogs with ventricular tachypacing–induced congestive heart failure. *Circulation*. 2001;104:2608-2614
146. Lim TK, Ashrafian H, Dwivedi G, Collinson PO, Senior R. Increased left atrial volume index is an independent predictor of raised serum natriuretic peptide in patients with suspected heart failure but normal left ventricular ejection fraction: Implication for diagnosis of diastolic heart failure. *European Journal of Heart Failure*. 2006;8:38-45
147. MacIver DH, Townsend M. A novel mechanism of heart failure with normal ejection fraction. *Heart*. 2008;94:446-449
148. Karamitsos T, Neubauer S. Cardiovascular magnetic resonance in heart failure. *Current Cardiology Reports*. 2011;13:210-219
149. Morris DA, Boldt L-H, Eichstädt H, Özcelik C, Haverkamp W. Myocardial systolic and diastolic performance derived by 2-dimensional speckle tracking echocardiography in heart failure with normal left ventricular ejection fraction. *Circulation: Heart Failure*. 2012;5:610-620
150. Phan TT, Abozguia K, Nallur Shivu G, Mahadevan G, Ahmed I, Williams L, Dwivedi G, Patel K, Steendijk P, Ashrafian H, Henning A, Frenneaux M. Heart failure with preserved ejection fraction is characterized by dynamic impairment

of active relaxation and contraction of left ventricle on exercise and associated with myocardial energy deficiency. *Journal of the American College of Cardiology*. 2009;54:402-409
151. Phan TT, Shivu GN, Abozguia K, Gnanadevan M, Ahmed I, Frenneaux M. Left ventricular torsion and strain patterns in heart failure with normal ejection fraction are similar to age-related changes. *European Journal of Echocardiography*. 2009;10:793-800
152. Gheorghiade M, Vaduganathan M, Shah SJ. Evaluative framework for phase ii studies in patients with heart failure and preserved ejection fraction∗. *JACC: Heart Failure*. 2013;1:123-126
153. Gottdiener J, Kitzman D, Aurigemma G, Arnold A, Manolio T. Left atrial volume, geometry, and function in systolic and diastolic heart failure of persons > or = 65 years of age (the cardiovascular health study). *Am J Cardiol*. 2006;97:83 - 89
154. Kurt M, Wang J, Torre-Amione G, Nagueh S. Left atrial function in diastolic heart failure. *Circ Cardiovasc Imaging*. 2009;2:10 - 15
155. Paulus WJ, Tschöpe C, Sanderson JE, Rusconi C, Flachskampf FA, Rademakers FE, Marino P, Smiseth OA, De Keulenaer G, Leite-Moreira AF, Borbély A, Édes I, Handoko ML, Heymans S, Pezzali N, Pieske B, Dickstein K, Fraser AG, Brutsaert DL. How to diagnose diastolic heart failure: A consensus statement on the diagnosis of heart failure with normal left ventricular ejection fraction by the heart failure and echocardiography associations of the european society of cardiology. *European Heart Journal*. 2007;28:2539-2550
156. Sanders P, Morton JB, Davidson NC, Spence SJ, Vohra JK, Sparks PB, Kalman JM. Electrical remodeling of the atria in congestive heart failure: Electrophysiological and electroanatomic mapping in humans. *Circulation*. 2003;108:1461-1468
157. Caldwell JC, Mamas MA. Heart failure, diastolic dysfunction and atrial fibrillation; mechanistic insight of a complex inter-relationship. *Heart Fail Rev*. 2012;17:27-33
158. BRUNS HA. Left atrial function studied by cineangiocardiographic volume determinations. *American Journal of Roentgenology*. 1970;110:467-473
159. Kroeker CAG, Shrive NG, Belenkie I, Tyberg JV. Pericardium modulates left and right ventricular stroke volumes to compensate for sudden changes in atrial volume. *American Journal of Physiology - Heart and Circulatory Physiology*. 2003;284:H2247-H2254
160. Schotten U, Neuberger H-R, Allessie MA. The role of atrial dilatation in the domestication of atrial fibrillation. *Progress in Biophysics and Molecular Biology*. 2003;82:151-162
161. Marcus KA, Janoušek J, Barends ME, Weijers G, de Korte CL, Kapusta L. Synchronicity of systolic deformation in healthy pediatric and young adult subjects: A two-dimensional strain echocardiography study. *American Journal of Physiology - Heart and Circulatory Physiology*. 2012;302:H196-H205
162. Nakai H, Takeuchi M, Nishikage T, Lang RM, Otsuji Y. Subclinical left ventricular dysfunction in asymptomatic diabetic patients assessed by two-dimensional speckle tracking echocardiography: Correlation with diabetic duration. *European Journal of Echocardiography*. 2009;10:926-932
163. Tan YT, Wenzelburger F, Lee E, Heatlie G, Leyva F, Patel K, Frenneaux M, Sanderson JE. The pathophysiology of heart failure with normal ejection fractionexercise echocardiography reveals complex abnormalities of both

systolic and diastolic ventricular function involving torsion, untwist, and longitudinal motion. *Journal of the American College of Cardiology*. 2009;54:36-46
164. Wang J, Khoury DS, Yue Y, Torre-Amione G, Nagueh SF. Preserved left ventricular twist and circumferential deformation, but depressed longitudinal and radial deformation in patients with diastolic heart failure. *European Heart Journal*. 2008;29:1283-1289
165. Dernellis Md JM, Stefanadis Md CI, Zacharoulis Md AA, Toutouzas Md PK. Left atrial mechanical adaptation to long-standing hemodynamic loads based on pressure–volume relations. *The American Journal of Cardiology*. 1998;81:1138-1143
166. Stefanadis C, Dernellis J, Toutouzas P. A clinical appraisal of left atrial function. *European Heart Journal*. 2001;22:22-36
167. Voskuyl AE. The heart and cardiovascular manifestations in Rheumatoid Arthritis. *Rheumatology*. 2006;45:iv4-iv7
168. Liang KP, Myasoedova E, Crowson CS, Davis JM, Roger VL, Karon BL, Borgeson DD, Therneau TM, Rodeheffer RJ, Gabriel SE. Increased prevalence of diastolic dysfunction in Rheumatoid Arthritis. *Annals of the Rheumatic Diseases*. 2010;69:1665-1670
169. Distler O, Pignone A. Pulmonary arterial hypertension and rheumatic diseases—from diagnosis to treatment. *Rheumatology*. 2006;45:iv22-iv25
170. Acar G, Sayarlioglu M, Akcay A, Sokmen A, Sokmen G, Yalcintas S, Nacar AB, Gunduz M, Tuncer C. Evaluation of atrial electromechanical delay and left atrial mechanical functions in patients with Rheumatoid Arthritis. *Turk Kardiyol Dern Ars*. 2009;37:447-453
171. Schattke S, Knebel F, Grohmann A, Dreger H, Kmezik F, Riemekasten G, Baumann G, Borges A. Early right ventricular systolic dysfunction in patients with systemic sclerosis without pulmonary hypertension: A doppler tissue and speckle tracking echocardiography study. *Cardiovascular Ultrasound*. 2010;8:3
172. Zhou W, Bovik AC. A universal image quality index. *Signal Processing Letters, IEEE*. 2002;9:81-84
173. Eskicioglu AM, Fisher PS. Image quality measures and their performance. *Communications, IEEE Transactions on*. 1995;43:2959-2965
174. Hudsmith LE, Petersen SE, Francis JM, Robson MD, Neubauer S. Normal human left and right ventricular and left atrial dimensions using steady state free precession magnetic resonance imaging. *J Cardiovasc Magn Reson*. 2005;7:775-782
175. Mininni S, Diricatti G, Vono MC, Giglioli C, Margheri M, Olivo G, Gensini G, Galanti G. Noninvasive evaluation of right ventricle systolic pressure during dynamic exercise by saline-enhanced doppler echocardiography in progressive systemic sclerosis. *Angiology*. 1996;47:467-474
176. Sengupta PP, Korinek J, Belohlavek M, Narula J, Vannan MA, Jahangir A, Khandheria BK. Left ventricular structure and function: Basic science for cardiac imaging. *J Am Coll Cardiol*. 2006;48:1988-2001